An Investigation into Reducing Time Dependent Creep of a Polyethylene Geotextile using Glass Fiber Yarns

By

Jun Xiong

A Thesis submitted to the Faculty of Graduate Studies of

The University of Manitoba in partial fulfilment of the requirements of the degree of

Master of Textile Sciences

Department of Textile Sciences

University of Manitoba

Winnipeg

Abstract

An investigation has been carried out to reduce the deformation behavior of polyethylene (PE) woven geotextile fabric by making PE fabric-glass yarn composite structure using stitching and laminating. The results showed that reinforcement significantly reduced the creep and IED as long as the tensile stress is lower than the total load bearing capacity of the glass yarns in the composite structure. However, the strength of PE-glass composite fabric was solely dependent on the strength of the glass yarns. The strength from PE yarns only contributes when all glass yarns are broken. Cast result of concrete columns using the glass yarn reinforced PE fabric by stitching method suggested that the glass yarn must face outside of the fabric formwork to avoid damage of both fabric surface and column surface.

Table of content

List of Tables

List of Figures

Acknowledgements

The author thanks Dr. Mashiur Rahman, Professor Mark West, Dr. Tammi Feltham, and Dr. Lena Horne for the technical support and thesis review.

The author tanks C.A.S.T. lab of University of Manitoba for the great training, learning and inspiring.

Also thanks to K9 Storm Inc. for the help of making glass yarn stitched PE fabric.

Chapter 1. Introduction

Glass fiber is perhaps the most commonly used reinforcing fiber among all technical fibers (Mukhopadhyay, 1993). Its advantages includes: high strength, high modulus, durable in many conditions (thermally stable, chemical resistant, resistant to weather and lights etc.), low cost and widely available. Polyethylene (PE) is the most commonly used textile material in geotextiles due to its low cost, tear resistant, light weight, chemical resistant and importantly, resistant to weather and insects (Rankilor, 2000). In this paper, plain woven PE geotextile is used in architecture application as a flexible formwork material to cast concrete. The process is in great success since using PE saves large amount of material cost, labor and time (Abdelgader, West, & Górski, 2008). Although, being a thermoplastic material PE is inherently ductile and can deform and creep considerately overtime and creates problems. Thus an investigation of using glass fiber as reinforcement on PE geotextile is designed. In the investigation, both the changes of the PE textile's mechanical property after reinforcement and the potential impact on the fabric-from work that use the reinforced fabric is evaluated.

1.1 Creep behavior of textile materials

The tensile strength of a textile is generally expressed in breaking load per linear density such as grams, pounds, or Newton per denier and per tex[1]; or in terms of tensile stress at break in Pascal or psi (pound per square inch). Young's Modulus, the ratio of applied force (weight or stress) over the elongation (extension length or strain ratio), is usually used to descript a textile's stiffness. Stress-strain curves are used commonly in the textile industry to describe a textile's strength and stiffness. The curve depicts the change of strain of a textile due to the change of

[1] Denier is measured as the weight in pounds of a textile per 9000 meters. Tex is measured as the weight in pounds of a textile per 1000 meters. 1 tex = 9 denier.

stress and is usually plotted by testing a textile under increasing tension force until it breaks. Figure 1.1 illustrates the stress/strain curve for some common fibers and some technical fibers. See from these charts, carbon fiber is the strongest fiber; glass fiber is the strongest common fiber; UHMWPE (Ultra High Molecular Weight Polyethylene) is the strongest organic fiber and polyester is the strongest common organic fiber.

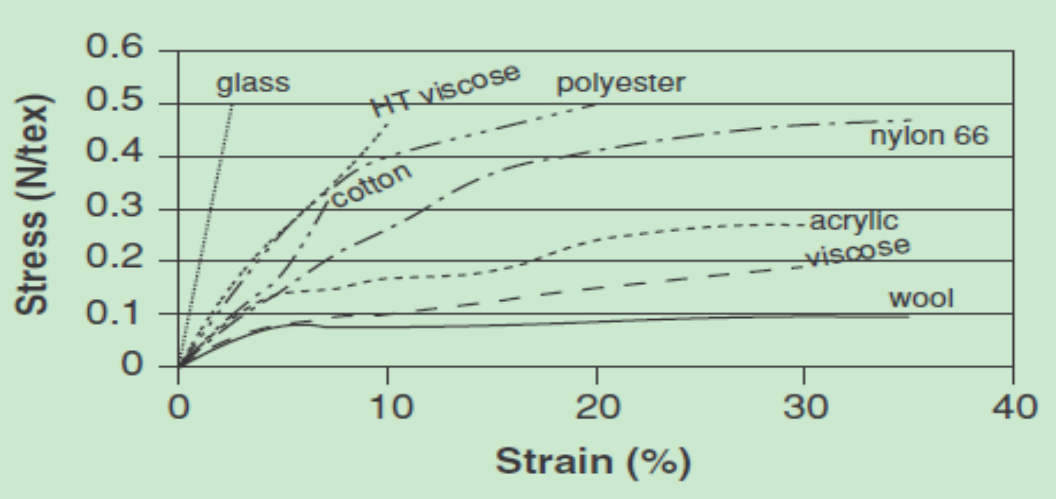

a)

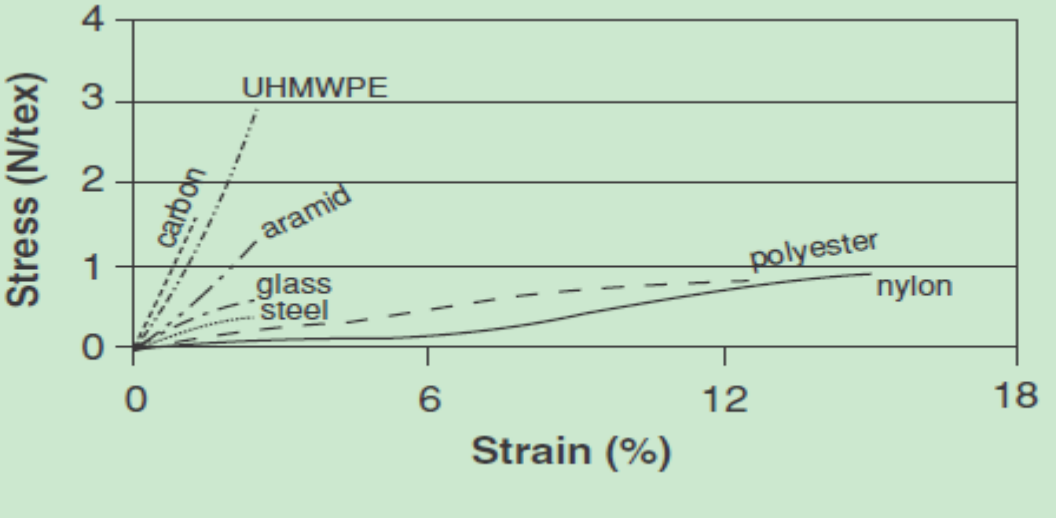

b)

Figure 1.1 Stress and strain curve of some common fibers and technical fibers. a) top, stress and strain curve of some common fibers. b) btottom, stress and strain curve of some technical fibers (Miraftab, 2000).

Stress/strain curves, however are inadequate on depicting the dimensional stability of a textile under stress over a long period of time. When applied with a constant load that is not enough to break the textile, textiles have tendency to elongate over time. Some of the elongation is recovered when the load is removed but some are not. This is a very important factor to considerate when using textiles as load bearing members. Figure 1.2 a) depict a typical creep behavior of a textile. At the beginning when the load is applied - point A, the textile stretched immediately (denoted as IED: Instantaneous Elastic Deformation) from 0 to 1. As time elapse, the textile continue to stretch slowly from 1 to 2 (creep) - point B. Then at point C, the load is removed and the textile bounces back from 2 to 3 (denoted as IER: Instantaneous Elastic Recovery). As time elapses again, the textile at point D, slowly shrink back from 3 to 4 but leave behind another portion from 4 to 0 unrecoverable. The slowly recovered elongation from 3 to 4 is called primary creep and the unrecovered portion from 4 to 0 is called secondary creep in most textile textbooks and papers. Figure 1.2 b) illustrates the elongation behavior of the textile in the loading process using strain/time curve. The initial elastic strain section in this curve represents the IED in Figure 1.2 a) which is a result of the elastic property of the textile (elastic implies recoverable stretch)[2]. Some of the elasticity is the result from the straightening of the fibers and yarns in the textile which were previously crimped during the yarn spinning, weaving or knitting process. Some is result from the polymer chain extension at the molecular level. When the load is removed, this portion of the stretch is largely recoverable depending on the resilient property of the textile. In next stage, the primary creep in the curve has a deep slop followed by a flattening turn. The beginning point of this portion is called the yielding point. This section

[2] The elastic behavior of a textile is rather complicated than simple. Especially polymeric textile materials that commonly exhibit unrecoverable stretch even under small stress. The mechnisim is due to the sliding, uncoilling or reorienting of the polymer chains. However in most fabrics that has manufactured through multiple stages of axial drawing process, this portion is relatively small compare to the recoverable portion.

accounts for some continued fiber and yarn reorientation in the textile as well as polymer chain extension. At the point where the curve flattened, the textile has reached a stable mechanical state that the fabric, yarns, fibers and polymer chains are tightened, and oriented towards the loading direction. The yielding strain is of particular interest of manufacturers as it determines the safety load at that strain for the textile if it is designed to sustain tension. Among common organic polymer fibers, polyester has the highest safety load at 60% of its maximum load; polyethylene and polypropylene are at 20% (Barbero, 2011). If the load continues to apply, the textile will undergo some internal structural change that polymers, fibers, and yarns have to reconfigure into a more efficient structure to resist the load. At a relatively low rate, polymers reorient, slide passing each other and unfold their chains on the direction of the load. This result an unrecoverable elongation called the secondary creep. If the load is not sufficiently high, the creep will not proceed further and the strain of the fabric remains stable for a long time. If the load is above this threshold, the creep will eventually proceed into the final stage of tertiary creep: a sudden accelerated strain rate followed by breaking of the textile. This is the result of the progression of the force accumulation at a weak point previously caused by thinning of the material in the secondary stage.

The test of tensile strength and modulus is fairly straight forward. A section of textile is clamped between two jaws and the load or strain is increased at a fixed rate until the textile breaks. The curve is obtained by connecting the data points. The test of creep involves a section of textile is applied with a constant load and strain is recorded at each time point until the strain stabilizes at a very slow rate (near zero) or until the specimen is broken. The specifications of these tests are specified in various standards such as ASTM and CGSB. Manufacturers and their customers negotiate terms for which to follow.

It is worth mentioning that sometimes the creep behaviors are expressed in the form of stress relaxation as illustrated in Figure 1.2 c). When a textile is applied with a constant strain, the stress decreases over time as the textiles are “relaxed”. The relaxation mechanism is same as described earlier that the textiles under load would reconfigure into a more efficient structure to cope with the stress.

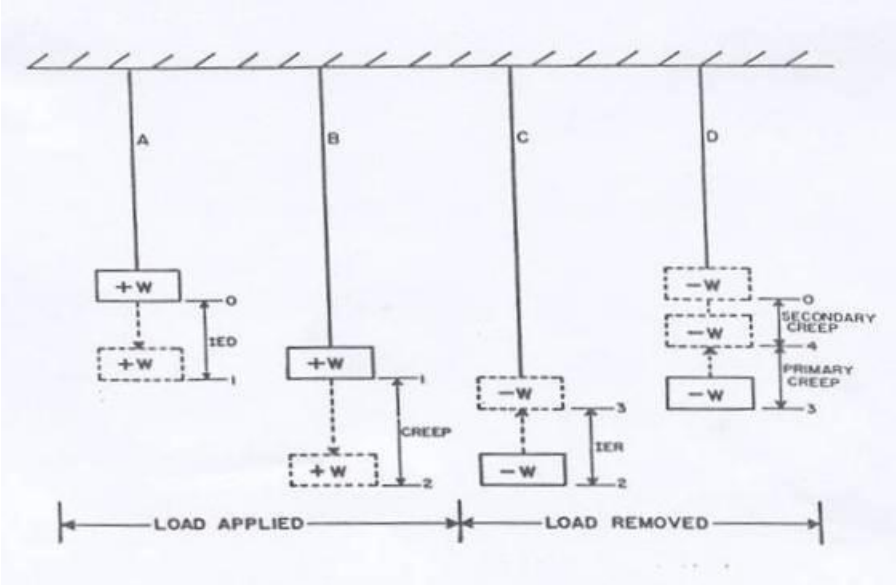

a)

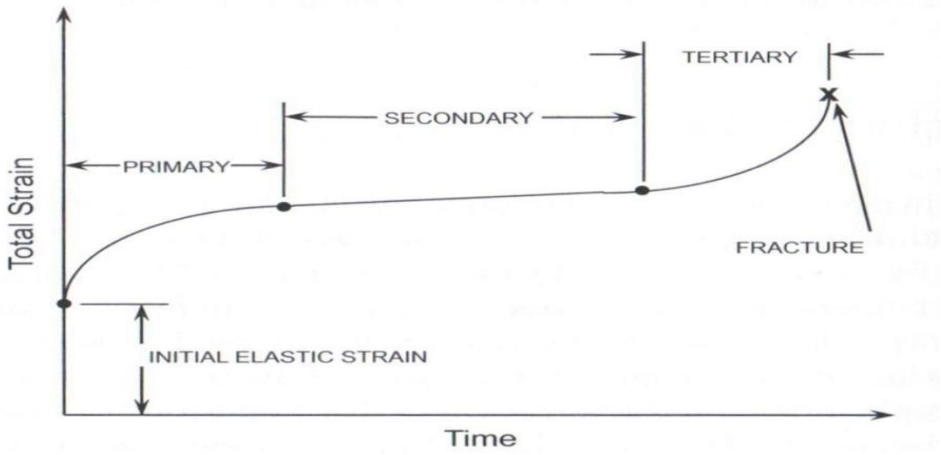

b)

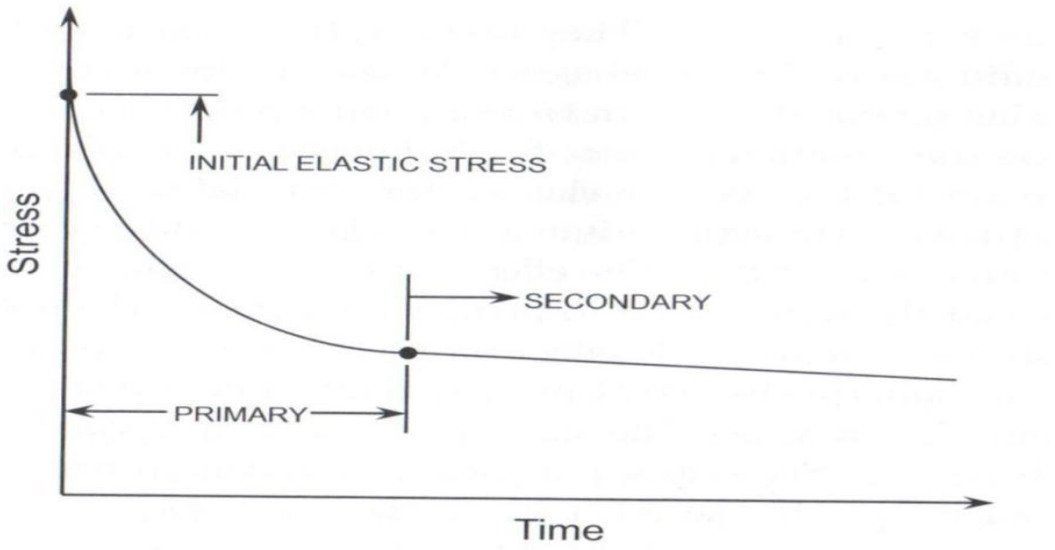

c)

Figure 1.2 Creep behavior of textile materials. a) top, Creep behavior of a textile (Adanur, 1995). b) middle, strain behaviour over time of a viscous material. c) bottom, stress experience of a viscous material over time on a constant strain level (Barbero, 2011).

1.2 Fabric formwork in architecture

Fabric formwork is a technology that uses fabrics to make molds for concrete casting. Compared to conventional molds that use lumber, plywood and steel, the molds made of fabrics are flexible, easy to use, light weight, permeable and cost less (Abdelgader, West, & Górski, 2008). The concrete cast from a fabric mold has a smooth surface that requires no additional polishing or coating. This is because when the wet concrete gets poured into the mold, air bubbles inside can be squeezed out through the pores between the yarns of the fabric. The conventional formwork, on the other hand, is impermeable and stops the air bubbles from escaping and creates blow holes and dents on the surface of the concrete (Figure 1.3). In addition, the permeability of the fabrics also allows water to be bled out by the hydraulic pressure of the wet concrete, thus reducing the cement/water ratio to a more suitable range so

when the concrete hardens the density and strength increases. It is reported that the concrete columns cast in a fabric mold can sometimes increase up to 100% of the compressive strength when compared to the ones that are cast in conventional molds (Pildysh & Wilson, 1983). The increased strength and density however is only found on the surface layer of the concrete. Therefore, the overall effect diminishes when the specific surface area decreases, e.g. an increase of the diameter of a column would result in a decrease of the strength difference of the ones cast in fabric molds when compared to the ones cast in conventional molds (Delijani, 2011). Never the less, a dense surface protects the concrete from erosion and abrasion, reduces permeability and thus, protects reinforcement steel from the penetration of chloride and carbonate ions (Marosszeky, Chew, Arioka & Peck, 1993). To be an effective fabric formwork, the selection of the fabric has to be specifically tailored to the project.

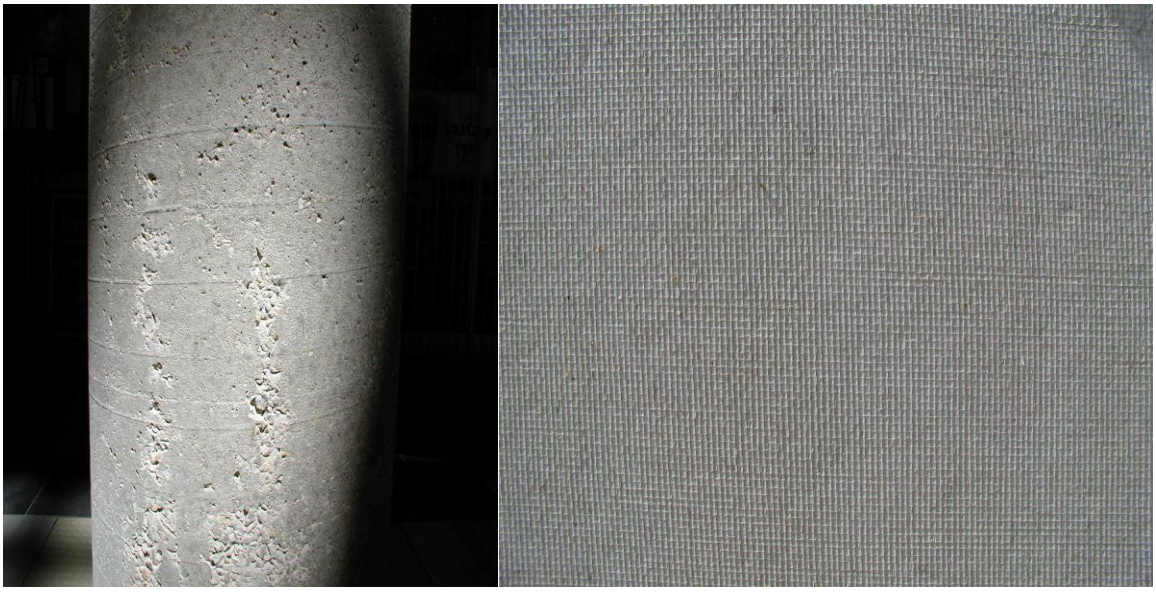

Figure 1.3. Resultant concrete surface cast in fabric formwork. Blow holes on surface of a concrete column cast in conventional mold (left) and surface of concrete column cast in fabric mold (right) (Delijani, 2010.).

In a typical fabric formwork project, the fabric used is preferred to be (Abdelgader, West, & Górski, 2008; Malone, 1999; Koerner & Welsh, 1980):

1. The fabric is strong enough to hold the pressure or the weight of the concrete.
2. The fabric complies with the designed shapes.
3. The fabric is permeable or impermeable depending on job requirements.
4. The fabric is fairly smooth so it will not adhere to, or be captured by the cured concrete.
5. The cost of the fabric is reasonably low.

Because fabric formwork is a relatively new field, there is no established standard and practice to select and use a fabric. In both academic research and commercial projects, professionals choose their own fabric based on their experiences, fabric availabilities, and personal preference. Thus, the reports on the quality and problems associated with fabric formwork have various results.

For example, in some experiments (Al Awwadi Ghaib & Górski, 2001), the compressive strength of concrete cast in fabric formwork did not increase significantly and even occasionally decreased. This is because the permeability of the fabric has a great effect on the resulting concrete. When the concrete is cast in the formwork, the water has a limited time to escape. As soon as the surface is cured, the water contained beneath can no longer leak out. Therefore, if the fabric is too tightly woven, the holes between the interlacing yarns will be too small to allow a considerable amount of water to pass through before the concrete surface is hardened. On the other hand, if the fabric is too loosely woven and has large holes, the cement in the concrete would bleed out with the water together and reduce its content in the concrete thus producing poor quality.

Ideally, a fabric mold should have pores that maximize the water flow and retain cement particles. Unfortunately, the particle sizes in a concrete mix vary greatly. In a study of the permeable filter medium of concrete casting, the author reported that the particles of their ordinary Portland cement range from 5μm to 500μm (Schubel, Warrior, & Elliott, 2008). In this study, the fabric was chosen according to their pore size distribution study which revealed that pores around 23μm would retain 95% of the particles. The authors cast the concrete in the fabric with pore at this range but the results showed no significant improvement of surface strength except the smoothness of the concrete surface were greatly improved and were free of blow holes. Perhaps if the fabric was tighter so that lesser particles would escape or if the fabric was actually more open so that more water could bleed out, the strength would be increased. Similar to this experiment, a widely adopted practice in geotextile to select appropriate fabric may also give us some insight. When water flows through the soil, most fine particles in the soil would be filtered and retained by the mass itself and only a small portion is released through the fabric pores. To match a textile for the soils, the pore distribution of the fabric should be that 90% of the pores are smaller than the top 10% the largest particles in the soil (Rankilor, 2000). This practice allows sufficient soil protection and water flow. Additionally, under less demanding hydraulic condition (low pressure or low flux rate), a geotextile can have pore sizes up to 5 times larger to allow more water to bleed and still be an efficient filter medium. Perhaps the same procedure can be applied in selection of the fabric for concrete casting once the particle size and pressure conditions are established.

Another fabric selection method is interestingly simple and intuitive. In Delijani (2010)'s master thesis "The Evaluation of Changes in Concrete Properties Due to Fabric Formwork," the selection of the fabric was done by a precast trial in which concrete was cast on an apparatus

having different available fabrics assembled on the bottom in separate cells (Figure 1.4). The weight of water and cement which leaked through these fabrics was collected and analyzed. The fabrics which produced high water leakage and low cement leakage were then chosen in later trials (Delijani, 2011). This method is particularly suitable for researchers and workers to pick a best match fabric from the market when a new custom made fabric is hard to obtain.

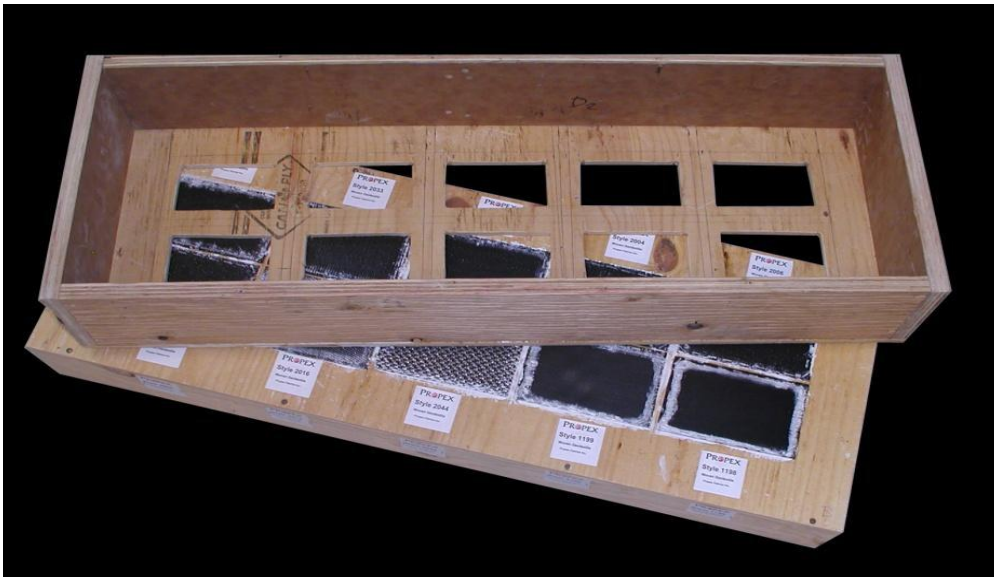

Figure 1.4. Wood frame with cells of testing fabrics (Delijani, 2010.).

In the field of technical textiles, synthetic fibers are most popular because of their high performance and low cost. Polypropylene and polyethylene are both strong fibers and have high chemical resistance, and they do not breakdown easily in the soil. If treated with proper finishing, coating or dies, they can also last very long in sunlight and many hazardous conditions (Fung, 2002). However, their thermal instability restricts them to be used only in low temperature operations. Polyester on the other hand is thermally stable with a glass transition temperature[3] at 70° C high and it is also stiffer, stronger and fairly chemical resistant but

[3] The temperature of a polymer between its glass state and melting state. Above it the amorphous region of the polymer has freedom to move but crystalline region remain rigid. Within this temperature, the polymer is viscouse (Hall, 2000).

susceptible to high alkaline environment. Nylon is another popular fiber with much higher elasticity. These fabrics are expected to resist abrasion force for its ability to stretch and recover; but in the wet environment it tends to soften (Rankilor, 2000).

Some vegetable fibers have comparable strength to synthetics; hemp, flax and jute are all strong and stiff fibers. The fabrics made from these fibers can be used as alternatives to synthetics in virtually all areas as long as the long term serviceability is not critical. In a test conducted at The Institute Textile de France (prior to 1988), a flax fiber extracted directly from an untreated plant showed comparable strength and stiffness in the same magnitude of Kevlar – a high strength, high modulus fiber commonly used for high performance textile such as bullet proof armor (Leflaive, 1988). Also, the strength and stiffness of flax fiber (as well as many other natural cellulous fibers) increases when wet, making it ideal for operations in moisture conditions (Mitra, 2002). In many developing countries, synthetic fabrics are too expensive, natural fiber fabrics are much cheaper and widely available. The cost to harvest and process them is economical in these countries where labor is abundant and local communities rely on the industry to bring income to their families (Pritchard, Sarsby, & Anand, 2000).

From the published literature, the formwork fabrics used are mostly woven. Compared to knits, woven fabrics have advantages in strength, stiffness and smoother surface. The tight yet moderately porous constructions also make them suitable for concrete casting. Even though the stretch ability of knits sometimes make them ideal to cast shapes with dramatic bends or folds, they do not have the required controllability of woven fabrics for jobs that require precise dimensions (e.g. columns and slabs). Knits are also easily caught in dried concrete because their loops make the fabric surface uneven. Nonwovens have been commonly used as filter mediums or absorbent liners inside a rigid mold to assist with the removal of excess water (Lawrence &

Shen, 2000), when used in a fabric-formwork, because of its isotropic fiber arrangement, there is a lack of shear defer from conventional woven and knit fabrics, it behaves more like papers and plastic sheets that normally creates wrinkles on the surface of cast object (See Figure 1.5). In nonwoven fabrics, each fiber is fixed in position with no room to move as they are mechanically, thermally or chemically bound together. The wrinkles are results of the inability of the nonwoven to shear planar to accommodate the opposing force. Nevertheless, these wrinkles may be an advantage in some cases where they are considered an interesting feature of the structure.

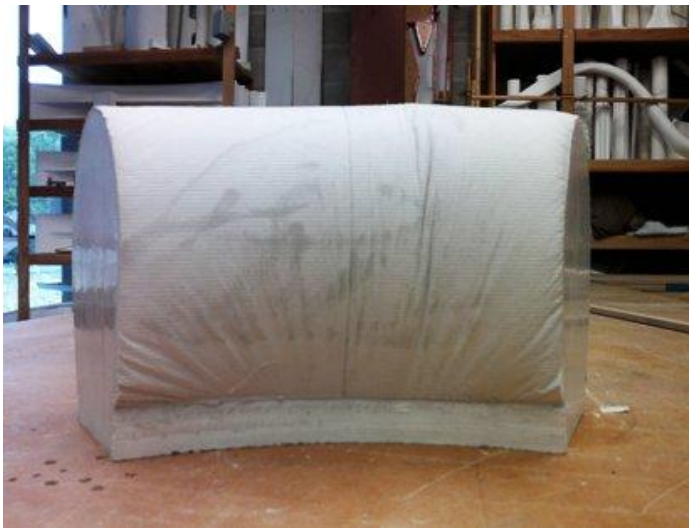

Figure 1.5. A sample casted in nonwoven fabric at the CAST lab during a trial cast (Copy right by Xiong, J. @ 2012).

1.3 Development of fabric formwork

The usage of fabrics and other textiles in construction jobs have a long history dating back to Roman times. Roman architect and engineer Vitruvius filled reed baskets with clay and spread it on top of the centering of the retaining walls in an underground structure. When the concrete was cast and hardened, the reeds that were lain in-between allowed for easy removal of the frame. To construct vaults in another underground project, he described a method to tie reeds together to make a scaffold where sand mortar could be applied to form the base for the casting

of the concrete. It is believed that reeds served as a cheap and easy alternative in those jobs where conventional formworks were too difficult to reach underground (Pollio, 1960).

Despite the long history in architectural experiences with textiles, scientific studies and documentations of the usage of fabrics in construction projects are very limited. The first documented patent of a fabric formwork was filed in the U.S. in 1899. Gustav Lilienthal (1849 – 1933) invented a fabric-formed suspended floor system that used impermeable fabric draped over beams for the casting of wet concrete with imbedded wire mesh. This patent is credited for savings on materials and labor. The floor is also described as having an interesting surface similar to a sofa cushion (Figure 1.6) (Lilienthal, 1899). Later, in the 1930s James Hardress de Warenne Waller, regarded as the most prolific inventor in the field of fabric formwork, patented several applications of fabric formwork: fabrics made from vegetable fibers were used as part of the casting mold to make floor systems similar to Lilienthal's. Fabrics were made into parallel encasing panels to cast walls, fabric sleeves were used to cast columns and fabrics liners were used to level the surface of canals, dikes and ponds. The usage of fabric in these applications would make the job easier, cheaper and faster. Waller's most important contribution in architecture, however, would be the invention of fabric formed Cteshiphon shell structures. These structures take the shape of inverted catenary arches to form steel scaffolds and hessian fabrics are draped over and applied with cement to harden into solid covers (Waller & Aston, 1953). In the time when resources were limited, because of the simplicity and low requirements of materials and labor, the Cteshiphon system was applied globally to build houses, storage units and factories during World War II up until the 1970s (Figure 1.7).

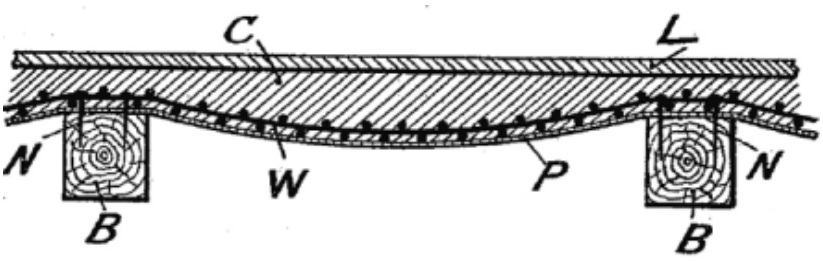

Figure 1.6. Lilienthal's floor system (Lilienthal, 1899.).

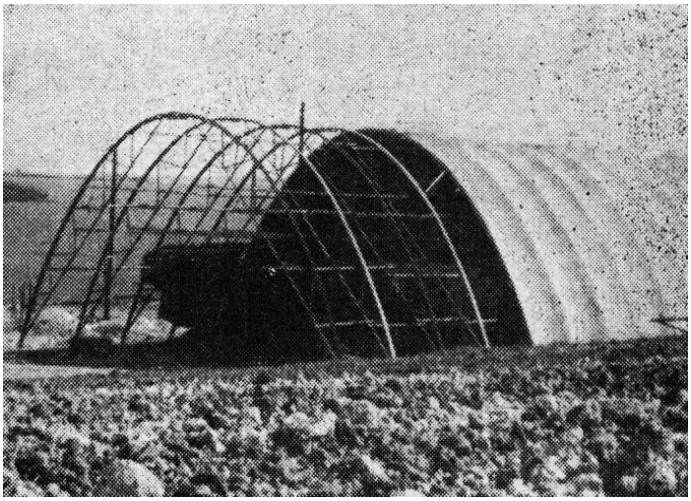

Figure 1.7., Cteshiphon shell (Waller, & Aston, 1953.).

At approximately the same time, the advantage of fabric permeability was noted and appreciated by Karl Billner who used a vacuum apparatus to suck out excess water from concrete through a fabric cover and the concrete was rendered with a surface with higher strength and less blow holes (Figure 1.8). His method was patented in 1936 in the US (Billner, 1936). Soon after, builders and researchers began to investigate the effect of fabric's permeability on concrete. Eduardo Bindhoff carried out a series of examinations of concrete's compressive strength cast in both fabric formwork and conventional formwork in his master's thesis in 1968 and reported that the compressive strength of concrete cast in fabric formwork was about 70% higher than the

concrete cast in conventional formwork due to the reduction of the water/cement ratio (Lamberton, 1989).

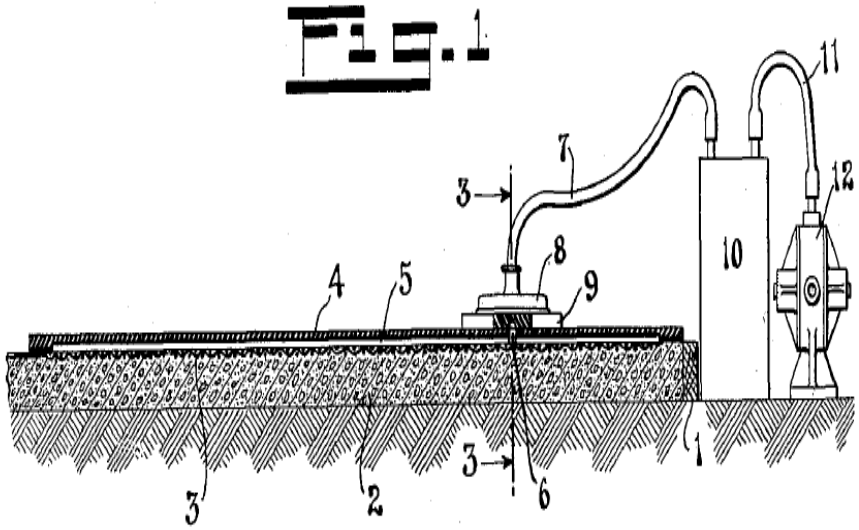

Figure 1.8. Vacuum treatment of concrete (Billner, 1936.).

The inventions and developments of synthetic fiber during the 20th century gave a boost to fabric's technical applications in architecture and civil engineering. Fabrics made from nylon, polyester, and polyolefin fibers are cheaper, stronger, and highly resistant to chemicals, insects, and micro-organisms. These fabrics can be used as roadway separation sheeting where a layer of fabric is placed between coarse gravel and fine grain soil to prevent the large gravel penetrating into the lower level soil and sinking the road surface. They can also be used as embankment lining to prevent soil loss while allowing the water to bleed out. Additionally they can be used to construct bank enforcement, pipeline foundations, and cavity fillings where other methods cannot be applied easily (Malone, 1999). In 1982, Bindhoff and King (1982) reported a rehabilitation project in Chile near Talcahuano where pile foundations of the Huachipato Pier were covered by Nylon jacketing and filled with concrete. The piles were first encased by wire

cages, then covered by Nylon jackets with zipper closure and pumped with a concrete mixture. Because of the higher pressure inside the concrete, excess water was purged out and the concrete hardened into an enforcement crust while the fabric was left on. The dense surface of the fabric-formed concrete efficiently protected the piles from erosion and the fabric sheath gave additional protection again abrasion. The project was reported to be in excellent condition six years after installation (Bindhoff & King 1982). In 1983, Pildysh and Wilson reported the very first installation of a fabric-formed concrete lining for a slope protection project in North America at Sundance and Keephills Thermal Generating Station in Alberta, Canada. In this project, a double layered synthetic fabric envelope was placed on the dike of the station and then pumped with concrete. The fabric allowed easy laying, covering and manipulation on the slope and held the liquid concrete mix in place while water was let out to allow curing. Consequently, a thin layer of concrete with high density and high strength was cast. The project was described as efficient and low cost with high quality (Pildysh & Wilson, 1983).

While the permeability of fabrics is utilized by builders and engineers, impermeable fabrics have also found their place in architecture. Wallace Neff in 1943 patterned his technology to build a concrete bubble house using inflatable domes. In his application, a rubber impregnated fabric was inflated to form a bubble shaped support and then a thin layer of concrete was sprayed over to harden into an erected base. The fabric was then removed to make another house while the first one was under completion. In the proceeding process the thin shell concrete base was hooped by horizontal steel rods like barrels and thickened in further casting. The houses were said to be effortlessly beautiful with flowing lines and curves, Figure 1.9 (Neff, 1941).

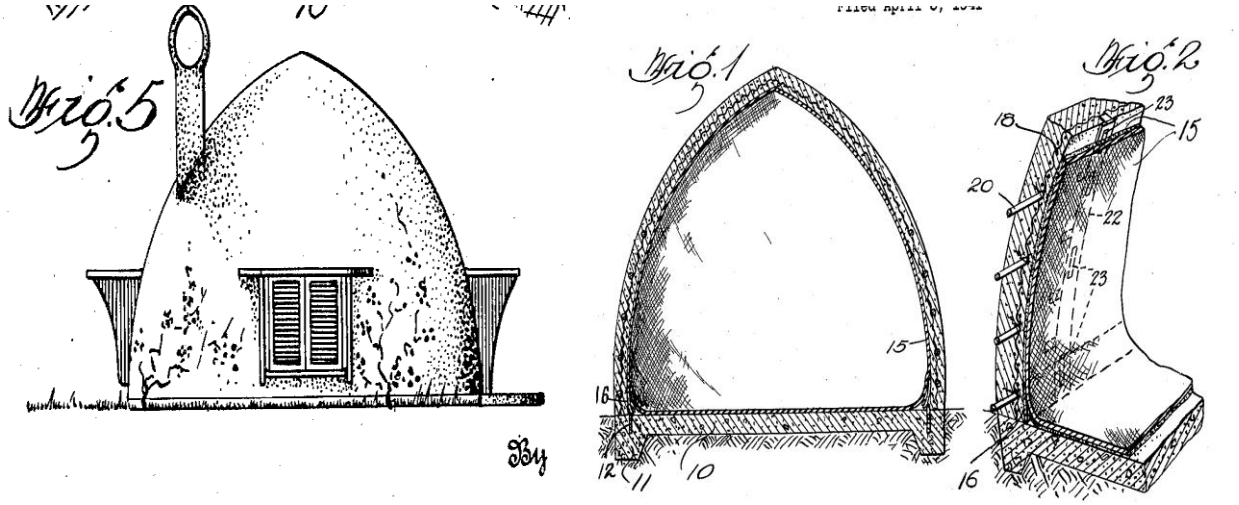

Figure 1.9. Concrete bubble house using rubber coated fabric (Neff, 1941.)

The aesthetic finish on concrete rendered by fabric formwork was acknowledged and explored by the famous Spanish architect Miguel Fisac. He employed the fabric's ability to form tactile shapes when respond to external forces and built magnificent structures with unique surface couture. In his project to build Yabarra Hotel Tres Islas in 1972, the façade of the building was left with beautiful impressions of plastic sheets and tying ropes. When the investors of the hotel saw it, because the surface was so vivid, they thought the plastic was still on the concrete (Figure 1.10) (Galiano, Frenneth, & Mostafavi, 2003)!

Figure 1.10. Façade of Yabarra Hotel (Galiano, Frenneth, & Mostafavi, 2003.).

Beside the advantages in construction simplicity, cost efficiency, improved concrete quality, and beautiful surface finishes, recent studies and practices have begun to incorporate the form-finding ability of the fabric into the design of the architectural projects. Fabric as a flexible, flowing material can be manipulated into various shapes and curves. This enables architects to build interesting structures. Examples can be found in many places. Students at the Architectural Association in London produced a set of sculptures with plaster and Lycra called "Grompies" (Figure 1.11). These sculptures used computer predicted patterns to stretch, stitch and anchor the Lycra fabric into a wooden frame, and then filled them with plaster. The weight of the plaster stretched out the fabric and cured into fascinating shapes.

Figure 1.11. Grompies (Carlin, 2010.).

(Pictures reproduced under permission from dezeen.com.)

Many other architectural institutions also explored the possibilities with fabrics and built walls, slabs, columns and furniture that are vivid, organic and conceptually challenging (Holzwart *et al*. 2010; Remy & Veenhuizen, 2010; Linssen, 2008; Manelius, 2009).

Today, more and more construction companies have begun to appreciate the utility and beauty brought by fabric formwork.

Fab-Form Industries Ltd. is a company in Canada that sells fabrics for concrete casting. Their product Fastfoot® is a membrane that can be installed under the wall to form a mold for the casting of footing and Fast-tube® is a coated woven polyethylene fabric folded into tubes to cast columns (Figure 1.12). By using their product, the jobs will be much easier than building lumber panel molds or using cardboard tubes, saving time and money (Fab-From Industry LTD, 2011). Another company, Concrete Canvas, sells a product wherein a layer of dry concrete mix is enveloped between a layer of woven fabric and a PVC membrane. This product can be laid anywhere into any shape and upon spraying with water it hardens to concrete. The company has successfully applied their products in the areas of ditch lining, slope protection, roofing and many other places where needed (Concrete Canvas, 2011).

Figure 1.12. Casting using Fastfoot® (left) and Fast-tube® (right) (Fab-Form Industry LTD., 2011.).
(Pictures reproduced under permission from Rick Fearn.)

1.4 The C. A. S. T. lab

The developments and knowledge of fabric formwork are intermittent and scattered among builders and architects. In 2002, Mark West, an architecture professor at the University of

Manitoba opened the Center for Architectural and Structural Technology (C. A. S. T.), dedicated to research fabric formworks. C. A. S. T. and Professor West, together with his colleagues around the world applied the principles of fabric formworks to cast objects that are both structurally efficient and sculpturally aesthetic. They saved tremendous time, labor, cost and materials that would have been expended in a conventional method. In the Canwest Global Theatre project in 1999, they used fabric formwork to build columns that have "bubbles" (Figure 1.14). In this project, a casting mold was made by folding double layered rectangular fabrics into cylindrical tubes. These tubes had a non-stretchable jacket and a stretchable spandex liner. The "bubbles" were formed by cutting holes on the jacket and allowing the liner to expand under the pressure. A couple years later in 2001, they employed similar methods on the island of Culebra, Puerto Rico to build columns for Casa Dent, a private villa. Thirteen columns ranging from 2.9m to 3.8m high were built from fabric formworks. These fabrics molds were designed and manufactured in Winnipeg, Manitoba and brought to the island of Culebra as luggage via plane in 3 small bags (West, 2004). In 2009, the C. A. S. T. lab invented and developed a method for Byoung Soo Cho architects in Soul, South Korea to build tilt-up façade walls. These walls have a weave like surface formed in a mold that had fabric going up and down on bundles of steel pipes.

Figure 1.13. Columns cast by CAST lab.

(Pictures reproduced under permission from CAST).

Beyond the cost saving and sculptural exploration, C. A. S. T. lab, led by Professor West also investigates the efficient structures that can be found in textile materials. Fabrics are fascinating in their ability to form drapes, folds and curves that are both aesthetic and structurally meaningful. The shape of a free hanging fabric is exactly the shape that distributes the tensile stress to hold its weight without any compressive or bending force. The catenary curves formed by horizontally hung fabrics can also be inverted to vaults that efficiently distribute compressive stress of the arches' own weight (Otto & Nerdinger, 2005). In equivalent strength, the beams and slabs in these shapes use much less materials and have much less weight than conventional shapes (e.g. orthogonal and cylinders).

The spirit of C.A.S.T. lab is inspired by the beauty of nature. No one can deny that nature is the best architect; from the wings of insects to the bones of animals, from membranes of a

soap bubble to the branches of trees, every bit of material and construction are perfectly beautiful and functional. The lines, curves, bends, and crinkles etc. formed in fabric formwork are all results of naturally occurring events. Professor West described these shapes as: "they are everywhere and they are beautiful, you will never get tired of them. They are not like fashion which comes and goes, they are independent of time, whether you look at them a hundred years ago or a hundred years later, they are always there and fascinating". Frei Otto, in his book "Light Weight Structures" described that extremely efficient, true minimum constructions are in harmony with, rather than in opposition to nature (Otto & Nerdinger, 2005).

1.5 Demand for improvement

Nevertheless, as mentioned in the beginning, textiles used in fabric formwork are not always suitable for the casting job. The PE fabrics, which are used extensively in construction and civil engineering applications, have disadvantage in creep resistance. In fact, Mr. Rick Fearn, the president at Fab-Form Industries Ltd, complained that their fabric formwork, the "Fast Tube", was stretching when casting large diameter columns. He reported that his polyethylene fabric would stretch to 19" in diameter at the bottom when casting a 16" diameter column. (R. Fearn, personal communication, January 13, 2012). A low cost, flexible and permeable textile with stiff tensile property is needed to improve the capability of fabric-formwork.

The proposed method to improve the PE fabric is to embed high stiffness and creep resistant yarns into the fabric matrix - a very common method used in composite enforcement (Barbero, 2011). Because stress always primarily accumulates on the stiffest structural member in a load bearing system, therefore, if reinforcement yarns with higher stiffness are imbedded

onto a PE fabric on the direction of applied stress, the burden of the tensile stress will shift from PE yarns to the reinforcement yarns so stretch and creep can be reduced.

The choice of reinforcement material is enormous thanks to the development of textile science. The next section is reviews of some most commonly used reinforcement textile materials.

1.6 Review of Some Technical Fibers

1.6.1 Carbon Fiber

Carbon fibers are consisted with at least 90% of carbon atoms crystallized and somewhat aligned in the fiber direction. Its atom arrangement is similar to graphite that each carbon atom is connected to 3 other carbon atoms with an σ bound and shared π bound cloud expanding the entire network (See Figure 1.17 a). The bound between these atoms are very strong but in graphite, these strong networks are stacked parallel to each other and bound by fairly weak Van De Vaal forces. Thus the normal graphite is soft and brittle. Carbon fiber on the other hand, has ribbon like graphite sheet aligned in the fiber axes direction (See Figure 1.17b). When subject to a tensile force, the close packed ribbons limits the sliding of each other holding the fiber structure without breaking or stretching until a cross sectional chain scissions of the graphite sheets propagates from a defected spot on the fiber surface (Bennett & Johnson, 1983). Because the fiber failure is closely related to its surface characteristics, carbon fibers that have smoother, less defected surface and more uniformed diameters along its axis are stronger. Without any defects, perfect graphite would have strength at 100 GPa and modulus at 1000 GPa. However, in the current manufacturing process, these defects are unavoidable and render the strength and stiffness of the produced carbon fibers to be an order of magnitude lowers. The strongest carbon

fiber produced so far had about 20 GPa in tensile strength and 680 GPa in modulus (Dorey, 1980) but Commercial available carbon fibers usually range from 1.5 GPa to 6 GPa in strength and 100 to 1000 GPa in modulus (Lysenko, Lysenko, Astashkina, & Gladunova, 2011).

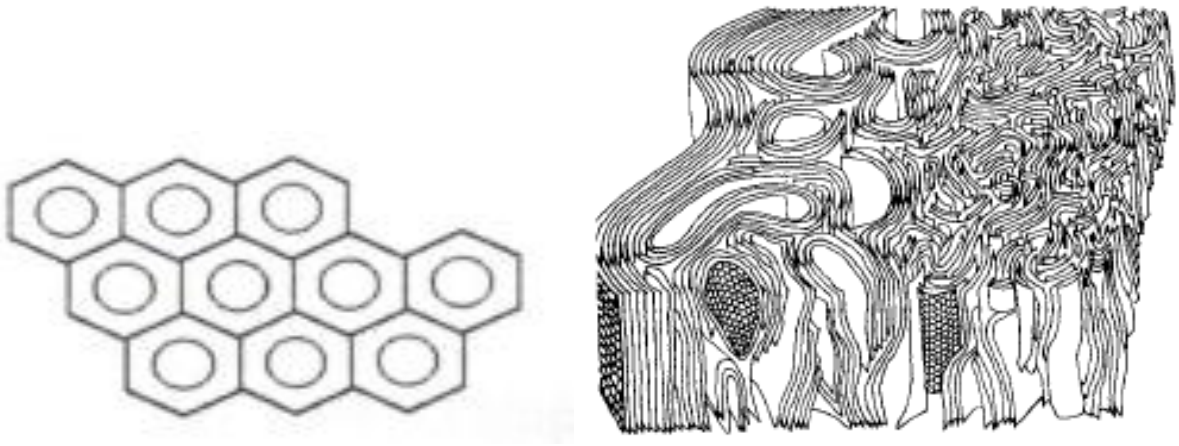

Figure 1.14. Carbone fiber structure. a) left, chemical structure of carbon fiber (Hall, Adanur, Broughton, & Brady, 1995.). b) right, mircroscopic structure of carbon fiber (Bennett & Johnson, 1983.).

The manufacturing process of carbon fibers is dependent on its precursors. Large variety of precursors are used to produce carbon fiber and PAN (polyacrylonitrile) is perhaps the most popular precursor, while mesophase pitch and cellulous fibers (rayon, cotton etc.) are also commonly used (Mukhopadhyay, 1993).

If PAN is used as the precursor, after the filaments is extruded 3 steps are needed to convert them into carbon fibers: 1. Oxidation at 200º C to 300º C, 2. carbonization around 1000º C to 1500º C, and 3. graphitized in between 1500º C to 3000º C. The process using pitch or cellulose fiber, such as rayon, is quite similar in all 3 steps except the oxidation involves more sub-steps at different temperatures. For pitch precursor, the commercial pitch is first polymerized to mesophase at above 350º C and then melt spun into fiber and thermal set before the carbonization. For rayon, the stabilization process goes through 3 sequences from low to high

temperature: 1. dehydrate the fibers at 25º C to 150º C, 2. dehydrate the cellulose molecular at 150º C to 240º C and then 3. aromatization at 240º C to 400º C.

The properties of the carbon fiber are partially related to its precursors as well as the manufacturing process (Mukhopadhyay, 1993). PAN based carbon fibers are usually produced to have high strength and pitch based carbon fibers are usually produced to have higher modulus while cellulose fibers are used to produce lower quality carbon fibers. Furthermore, the strength and stiffness of the carbon fibers can also be engineered during process by carbonization in different temperatures. High temperature treatment above 2000º C produces carbon fibers with high modulus and high strength carbon fibers are treated around 1500º C. Low modulus and low strength grade carbon fiber require no more than 1000º C.

In recent years, another carbon based material carbon nanotubes (CNT) is gaining popularity (Barbero, 2011). This type of material is consisted with carbon-carbon network wrapped into a tubular shaped nanofiber with nearly no defect on the surface. Due to this configuration, CNT can have strength and stiffness at 100 to 200 GPa and 0.5 to 1.5 TPa respectively. This material is now intensively researched to create supper strong and super lightweight composite materials in the hope to eventually make them more economical. However, the cost of making CNT is still very expensive and estimated around $500/gram.

Carbon fiber is the no.1 blessing for aerospace development. Its superior thermal insulation, thermal stability, light weight and high mechanical performance are crucial in the aviation industry. It is also being successfully used to make racing cars, racing bike, tennis rackets, golf clubs and many other sports for its cutting edge light weight advantage. Other important applications include architecture, mechanical engineering and medical textiles.

1.6.2 Glass Fiber

Glass fibers are filaments extruded from molten bulk glass which are obtained from melting a mixture of sand, limestone, and other oxide compounds. It is consisted with amorphous glass with silica content around 46% to 75% (Barbero, 2011). Unlike any other fibers, glass fibers are a truly isotropic material. The micro structure of glass fibers is no difference than a regular glass except their macro structures are in the fiber from. The atomic network consists of regions of crystallized silica as well as amorphous silica which the later are the majority and the rest are minerals and impurities. Its high strength mainly comes from its low defect surface and thus, it is best utilized in composite form when its surface is protected by resins such as epoxy (Miraftab, 2000). The strength of glass fiber range from 1.5 to 5 GPa and the modulus range from 55 GPa to 175 GPa (Barbero, 2011; Mukhopadhyay, 1993).

The properties of glass fiber can be manipulated with different mixture content (Mukhopadhyay, 1993). For example, S glass is a high strength glass fiber with tensile strength at 4.6 GPa and modulus at 86.8 GPa, it's content consists of 65% SiO_2, 25% Al_2O_3, and 10% MgO whereas regular E glass, with tensile strength around 3.5 GPa and modulus at 73.5 GPa, are made from 55.2% SiO_2, 14.8% Al_2O_3, 0.3% Fe_2O_3, 7.3% B_2O_3, 18.7% CaO, 3.3% MgO, 0.3% Na_2O, 0.2% K_2O and 0.3% F_2. AR glass, on the other hand is manufactured specifically for cement enforcement. It contains 16.7% ZrO_2, which can form a protective layer on the surface of the fiber against alkali environment when embedded in the cement. Its strength is similar to E glass but much stiffer with a modulus at 175 GPa.

Figure 1.18 illustrates the one stage, direct melt process to manufacture glass fibers. The ingredients are mixed, and transported into a furnace where molten glass are extruded directly

from spinneret and then cooled and winded. While other process such as two stage process, which the molten mixture are first cooled and stored in forms of marbles for later processing into fibers, are well established; the one stage process allows more efficient production.

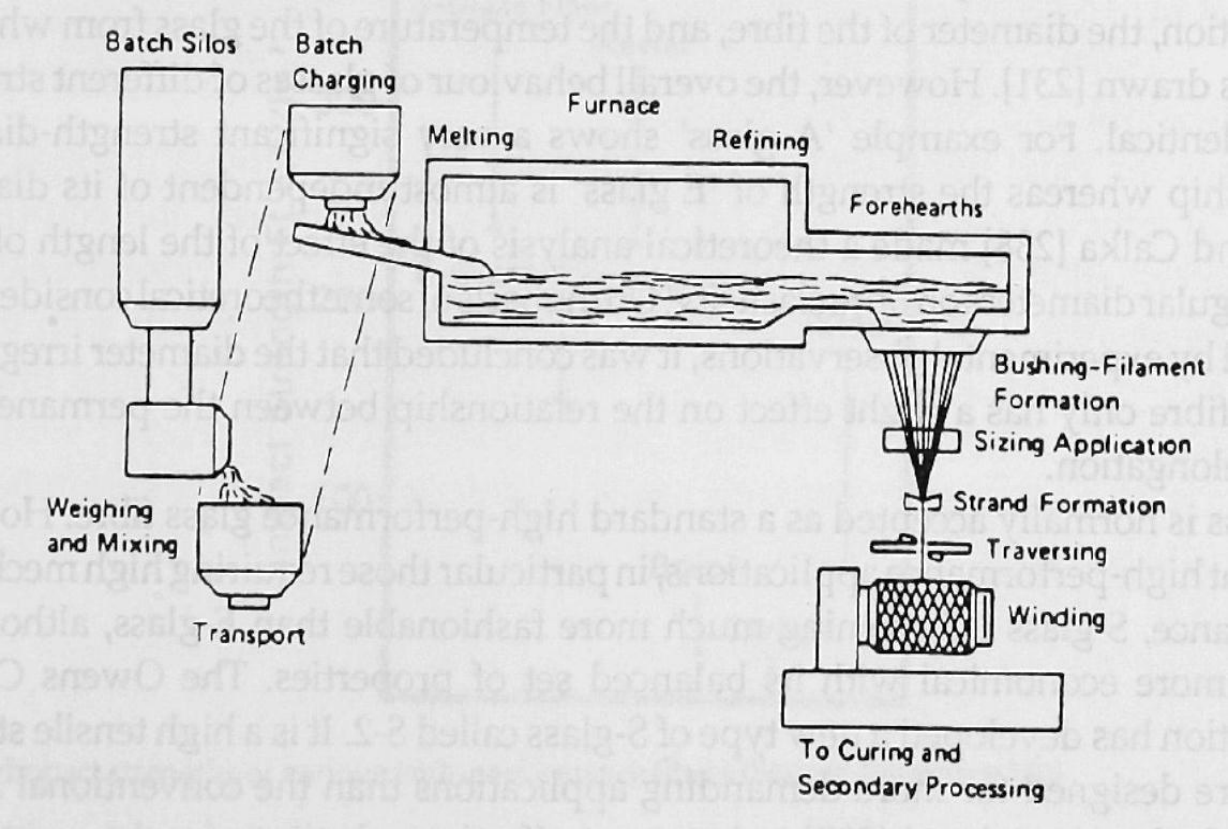

Figure 1.15. One stage, direct melt process manufacturing process of glass fiber (Mukhopadhyay, 1993.).

In addition to high mechanical properties, glass fibers also have good thermal insulation property and chemical resistant property. Its price is fairly cheap at about $1.6/kg. Compare to other materials, it is more cost efficient and is the most common fibers in low-cost industrial applications (Barbero, 2011). Among them, glass fiber enforced plastics is the most important application and are applied in many areas such as automotive, aircraft, civil and mechanical engineering and industrial components. It is also the primary substitute for asbestos because it does not present a health risk for the workers. Other important applications includes: flight deck amour, helicopter amour, seats, floors, and blades. Beside its mechanical, thermal and chemical

advantages, glass fibers are also made into optical fibers which can transmit signals with minimum loss (Mukhopadhyay, 1993).

1.6.3 Aramid Fibers:

Aramid fibers are long chain synthetic polyamide fibers which at least 85% of amide linkages are attached to two aromatic rings. Kevlar, Nomex are two common high performance aramid fibers manufactured by DuPont (Jassal, & Ghosh, 2001) (See Figure 1.19). Kevlar fiber have polymers of amide linkage attached to aromatic ring in "para" configuration resulted in higher strength and higher modulus whereas, Normex have "meta" linkage configuration result in higher heat resistance (Hall, Adanur, Broughton, & Brady, 1995.). Other manufactures such as Teijin also produces similar product under their brand name (e.g. Teijincorex).

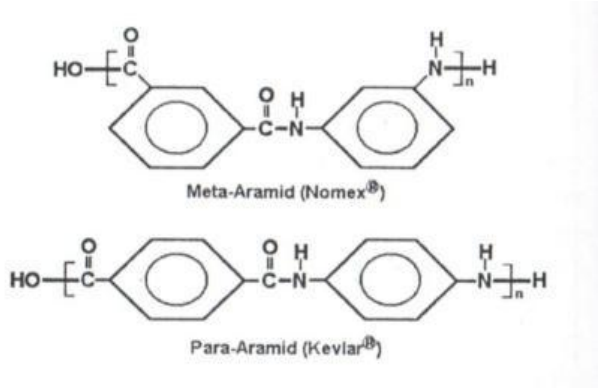

Figure 1.16. Chemical structure of Nomex and Kevlar (Hall, Adanur, Broughton, & Brady, 1995.).

Because aramid fibers are hard to dissolve and hard to melt, the commercial manufacturing of this type of fiber are not available until late 1990's when Kwolek, a researcher from DuPont, developed a method to synthesize high molecular weight lyotropic rigid chain poly (p-benzamide) with controlled crystallization in amide salt solvents (Kwolek, 1971). This development guaranteed DuPont a large leap in the market and it is still the number one producer of aramid fibers in the world market today (Jassal, & Ghosh, 2002).

The process to spin aramid fibers is different than normal fibers due to reasons mentioned earlier (Jassal, & Ghosh, 2002). This special solvent spinning process is called “gel spinning” in which the prepared solvent has limited viscosity. Aramid polymers are unlike to the normal aliphatic polymers. Due to its chemical structure, the polymer cannot tangle or coil in the solution state. Instead, they tend to align parallel to each other and from rod-like aggregates in random orientations and transfer to a liquid crystalline state at a critical concentration (gelation). In the polymerization state, molecular weight build up can be increased or decreased by choosing a suitable solvent which control the speed of gelation process. The polymers then go through washing, filtration and drying process to be cleaned before spinning. The second gelation process is introduced in the dope preparation process by re-dissolve the polymers in 100% sulfuric acid to form a viscose liquid ready for spinning. The weight concentration varies from 8% to 22% depends on the spinning temperature and method. Generally, wet spinning require lower concentration at low temperature and dry spinning require high concentration at high temperature.

During a wet spinning process, the disoriented crystalline domain orient along the fiber direction when the capillary shear force pulls the domain toward one direction and the filament attenuates under spinning tension, after precipitated in the air gap (about 1 cm) and the coagulations bath (also washes off the solvent acid), highly crystalline and highly orientated fibers are produced. The dry spinning process applies the same fiber forming strategy except the extruded fibers are coagulated in a counter stream of hot air which also evaporates the solvent. In 1999, Kawai patented a process which introduced a non-coagulation bath to stretch the spun stream of the solution and later draft the fiber in the coagulation bath to further improve the

orientation of the polymers and the fibers (Kawai, 1999). This process produced aramid fiber with tensile strength around 1.5 to 5 GPa and modulus from 200-500 GPa.

Commercial available aramid fibers have tensile strength and modulus range from 0.6 to 4.5 GPa and 17 to 145 GPa respectively (Jassal, & Ghosh, 2001). The regular DuPont product Kavlar 29 has tensile strength at 2.9 GPa and modulus at 70 GPa. It is much stronger and stiffer than most organic fibers and is comparable to glass fibers. Its strength and stiffness can be credited to its high molecular weight, high crystalline, high orientation and also its unique fiber morphology. Figure 1.20 shows aramid polymers lie in the fiber axis direction are bounded by hydrogen bounding across the axis and formed zigzag pleats along the fiber. This structure is extremely resistant to elongation and breakage as polymers are tightly locked into their position with no room to slide pass each other.

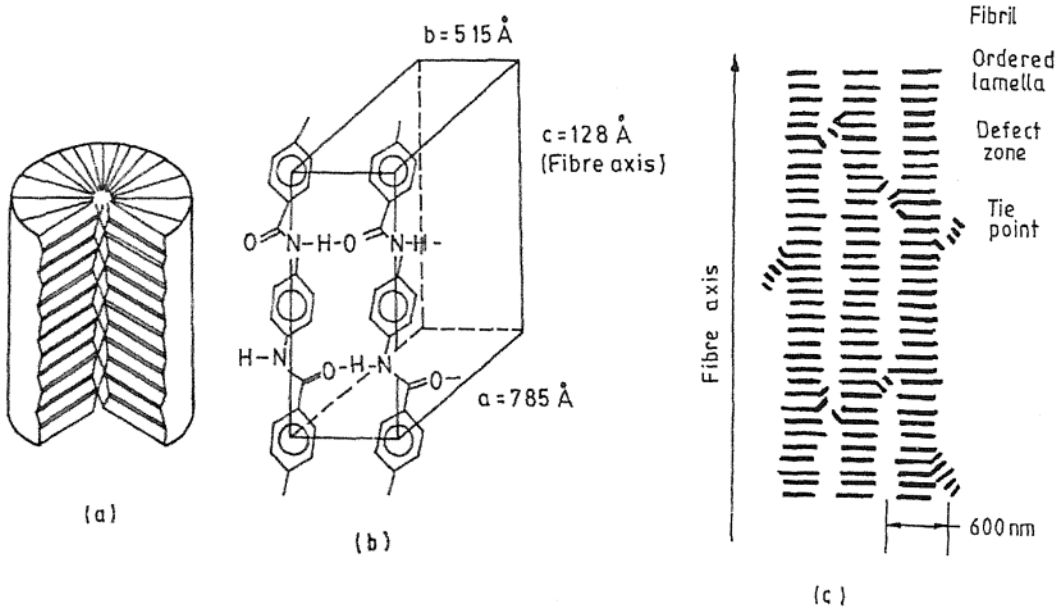

Figure 1.17. Microscopic structure of para-aramid fiber (Jassal & Ghosh, 2001.).

Because of its high mechanical performance as well as high tolerance to heat while being light weight, aramid fiber are used in many areas such as tire core reinforcement, bullet proof vest, fireman's jacket and composite for aircraft etc.

1.6.4 Polyolefin Fibers

Polyolefin fibers include polyethylene and polypropylene. This genus of fiber has the simplest chemical structure in organic fibers (Figure 1.21) and is also the lightest (both can float on water) and the most hydrophobic fiber. Regular polyolefin fibers are fairly strong already but somewhat elastic with a breaking elongation from 10% to 45% (Hatch, 2006). High performance polyolefin fibers are much stronger and much stiffer.

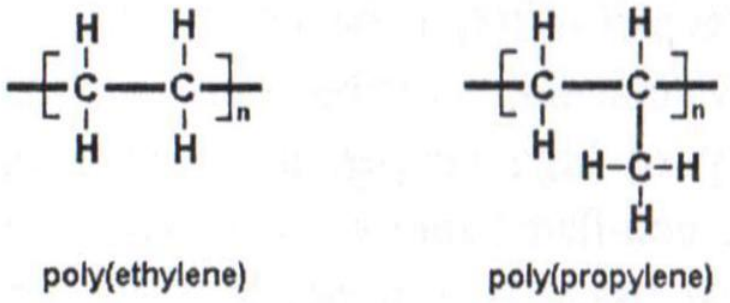

Figure 1.18. Chemical structure of polyethylene and polypropylene (Hall, Adanur, Broughton, & Brady, 1995.).

(UHMWPE: Ultra High Molecular Weight Polyethylene), produced by Honeywell International Inc. have tensile strength range from 2.61 GPa to 3.4 GPa and modulus from 79 GPa to 116 GPa (Karacan, 2005). This is comparable to glass fiber and aramid fiber, but from weight to weight ratio, it is twice stronger than aramid fiber and 15 times stronger than steel making it the strongest fiber known in the market (Happey, 1983). However, it is very sensitive to heat and it melts at 150º C and degrades at 350º C.

The superior strength in high performance olefin fibers is obtained by its extremely long and extended polymer chain with high molecular weight (more than 10^6 Dalton) high crystalline and high orientation. Huge amount of Van de Waals force is thus accumulated between these long chain interactions (Stein, 1988).

Two types of process are well developed to produce these fibers. Gel spinning and solid state drawing (Lemstra, Bastiaansen, & Rastogi, 2000). The Gel spinning is similar to that of described in aramid but involves multiple stages of gel drafting (Smith & Lemstra, 1980) (Smith, Lemstra, & Kiel, 1981). After spun from the spinneret the semi-solid filament are drawn in the cool water to unfold the polymer chain and align them to the fiber direction. In the next process the filament enters a hot draw oven to remove the solvent and further draw to its maximum draw ratio. The tensile force and modulus are found to have positive linear relationship with the draw ratio in Smith and Lemstra's experiment and the maximum strength and stiffness was achieved at draw ratio of 31.7 with 3.04 GPa tensile strength and 90.2 GPa modulus. The maximum draw ratio or the draw ability is influenced by the molecular weight and spinning conditions (Zhang, Xiao, Jia, & An, 1999; Smith & Lemstra, 1980; Mukhopadhyay, 2004). Higher polymerization increases the difficulty of draw ability and at some point inversely affect the quality of the final product. It is generally agreed that a moderate molecular weight with a narrow range of weight distribution is ideal for high drawing ratio and produces stronger fiber.

The solid state drawing, on the other hand, involves drafting melt spun or solvent spun sheet or filaments below its melting point in multiple steps. Many types of drawing techniques are available which include tensile drawing, constant load oven drawing, die drawing and zone drawing and zone annealing (Mukhopadhyay, 2004; Wu et al., 2003). Figure 1.22 shows drawing process of zone drawing and zone annealing. Initially the extruded sheet contains disoriented

amorphous polymers (isotropic). It is then stretched in horizontal direction and then zone-drawn in longitudinally at a very high ratio to orient the amorphous polymer. Subsequent zone-annealing at higher temperature increases the crystallization and more orientation.

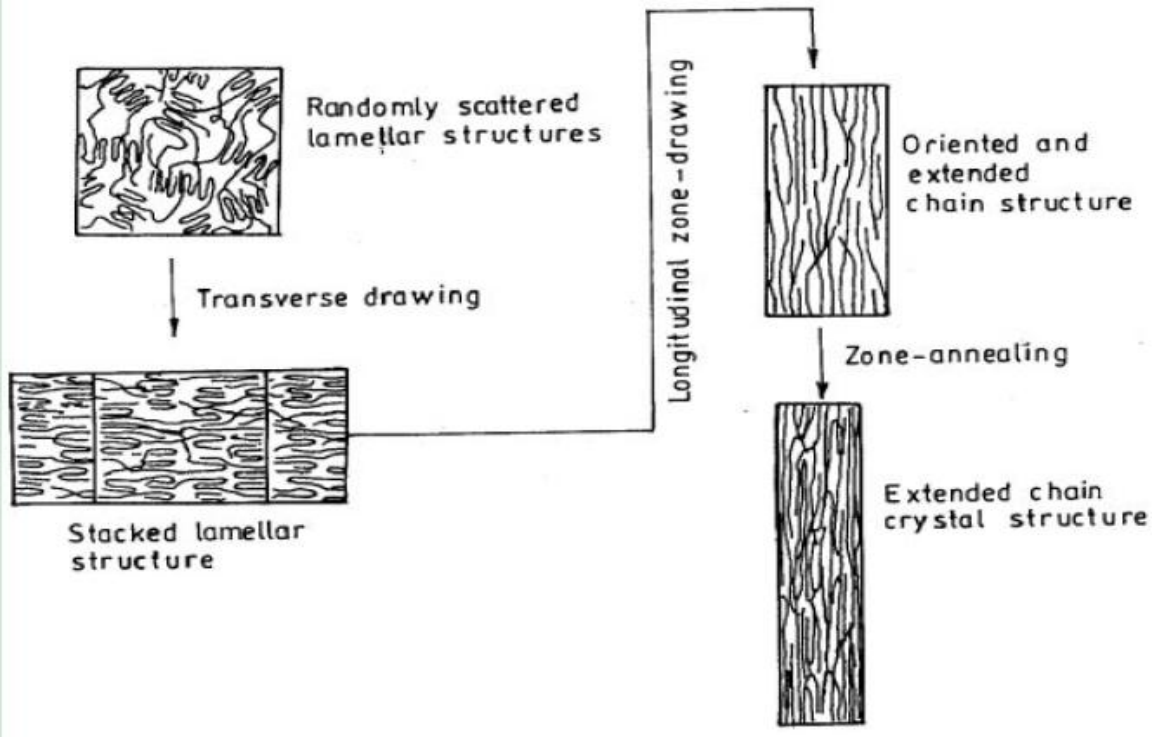

Figure 1.19. Microscopic structure during a zone drawing process of polypropylene fibers. (Mukhopadhyay, 2004.)

The applications of high performance polyolefin fiber include automobile, composite, and protection clothes etc. Its hydrophobic and low friction, high abrasion resistance quality made it the most popular material used in geo-textiles (Rankilor, 2000). Combination of these properties also made it popular in marine industry used in areas such as marine ropes and sailing boat enforcement (Pathasarathi, 2008). Moreover, its biocompatibility made it an important material in medical applications such as suture, joints and ligament replacement (Anonymous, 2007).

Chapter 2. Materials and Methods

Glass fiber is the stiffest and strongest fiber among the common fibers as shown in Figure 1.1 (a). Even though it is mechanically inferior when compared to those high tech fibers in figure 1.1 (b), its advantages in low cost and availability make it a better choice for fabric formwork applications because construction projects usually require large quantity and budget control. In this current study, two reinforcement methods of glass yarns on PE woven formwork fabric were investigated for deformation, one of them was laminated by a straight laid glass yarn (320 TEX) every half inch across the width of the fabric and the other was using 301 stiches at 6 per inch density to fix a glass yarn across the width at half inch interval.

One of the uniqueness of the reinforcement methods investigated in this study is that glass yarns were only introduced intermittently as reinforcement (every half inch) as oppose to using a whole sheet. This largely reduced the cost, weight and rigidity of the product. Another uniqueness is that the hosting base for the glass yarn reinforcement was a PE plain woven geotextile which is quite different than a impregnating plastic. The woven fabric is mechanically stiffer and stronger on their yarn directions but is less rigid and more flexible than a sheet of cured plastic. In addition, woven textile's permeability can facilitate concrete curing by bleeding water out during the hardening process (Lamberton, 1989). The third uniqueness is the method of stitching reinforcement where glass yarns were locked onto the base fabric via a simple, low cost process that is operable on any stitch machine.

In addition, since the stitching method altered the surface roughness of the base fabric, the effect on the surface of cast concrete was also investigated in the second set of the experiments through casting trails.

2.1 Materials

Polyethylene tape yarn fabric (Geotex® 315ST) was obtained from Propex (Chattanooga, TN, USA). C glass yarn (320 Tex) was obtained from Anping Furit Wire Mesh Making Co., China. Iron-on Clear Cover® (vinyl heat and bound) was obtained from Kittrich Corp. and polyester all-purpose sewing (top) thread was supplied by Coats and Clark (Greenville, SC, USA). Plywood boards for the fabric formwork and Quikrete® ready to use concrete mix manufactured by Target Product Ltd (http://www.quikrete.com/).

2.2 Reinforcing methods

Table 2.1 lists 6 groups of test specimens that are subject to two different methods of glass yarn reinforcement (one group is unreinforced original fabric) and two different testing loads.

Table 2.1. Reinforcement methods and Sample ID

Sample type	Reinforcement method	Applied load (N)	Samples ID
Original PE samples	N/A	500	O-500
Original PE samples	N/A	1000	O-1000
Glass yarn reinforced samples	Vinyl lamination	500	L-500
Glass yarn reinforced samples	Vinyl lamination	1000	L-1000
Glass yarn reinforced samples	Stitching	500	S-500
Glass yarn reinforced samples	Stitching	1000	S-1000

For both methods, the glass yarns were only introduced intermittently (every one-half inch). Theoretically, this would impart the necessary rigidity to resist deformation and avoid unnecessary cost.

A sequence of tests and experiments were carried out to achieve the research objectives. The first two tests were conducted to measure the tensile properties of the substrate and the glass yarns that were used as reinforcement. Afterwards, two separate experiments were carried out to assess the effective of reinforcing the substrate by laminating glass yarns onto it (Experiment 1) and by stitching the glass yarns onto it (Experiment 2).

2.2.1 Experiment 1 – Reinforcement by introducing laminating glass yarns

The purpose of this experiment was to reinforce the substrate by laminating glass yarns onto it. In an industrial setting, this process would be done in a more direct way with one layer of laminating material applied to the base fabric with glass yarns laid in between. Ideally, the optimum operating temperature and press time for the heat presser to laminate the glass yarns onto the substrate would be 143 Celsius for 15 seconds as established in trail experiments. However, the lamination for this experiment was undertaken by using a heat presser for which the temperature cannot be controlled as readily as with industrial equipment. If glass yarns were directly laminated on to the PE fabric using this heat presser, the PE substrate could melt under excessive heating or if the heating is not enough, the vinyl coating cannot be melted and laminated onto the substrate. These problems impact the testing quality and were hard to avoid using current equipment. Thus, the lamination process was performed in an alternative way to avoid heating the substrate directly.

To laminate the glass yarns, 6 strands of 320 Tex glass yarns were laminated inside two sheets of vinyl heat & bound (Iron-on Clear Cover® manufactured by Kittrich Corp) with two inch width as shown in Figure 2.1. Since the vinyl sheets were made from isotropic undrawn polymer, it can be assumed that its stiffness was low enough to not affect the composite's overall stiffness. With glass yarns sandwiched inside, vinyl sheets were pressed at about 143 Celsius for 15 seconds, cooled and then then cut into two 1 inches wide 10 inches long strips, each strip contain 3 glass yarns laminated inside. The stripes are then glued onto to the substrate (5 inches wide and 10 inches long) as shown in Figure 2.2.

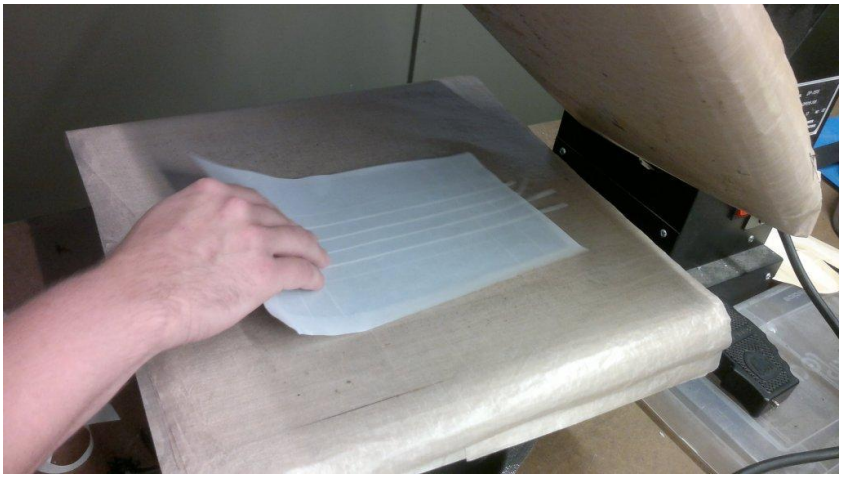

Figure 2.1. Press Machine for Vinyl lamination.

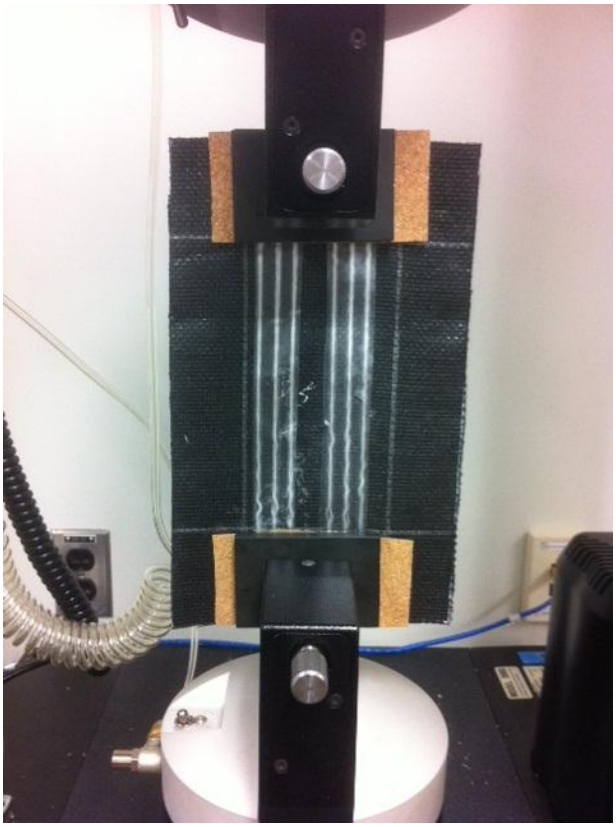

Figure 2.2. Laminated PE textile with glass yarn reinforcement mounted on Instron Tester.

2.2.2 Experiment 2 – Reinforcement by stitching glass yarns on substrate

A piece of Geotex® 315ST fabric (5 inches wide and 10 inches long) was reinforced by stitching 6 strands of 320 Tex glass yarns in the center section (3 inches width in the center) at 6

stiches per inch density along the length using a single needle, walking foot lockstitch machine (Brother model number: LS2-B837). The stitch pattern is classified as 301 stitches with the glass yarns threaded from the bottom bobbin and a general purpose polyester thread (all-purpose polyester sewing thread manufactured by Coats and Clark) threaded from the top needle. The stitched glass yarns were one half inch apart, laid on bottom side of the substrate and locked by the penetrating polyester top thread at each stitch loop. Figure 2.3 shows the yarn positions and the stitch pattern.

Figure 2.3. Glass yarns stitching reinforced specimen. The white yarns are glass yarns and black yarns (the black interceptions along the white glass yarns) are polyester yarns.

2.3 Test method

To investigate the effectiveness of the two types of reinforcement on reducing total elongation, IED and creep, tensile properties related to these 3 parameters of the reinforced

samples need to be tested and then compared to the test results from original samples. A tension creep test specified by ASTM D5262-07 is an adequate technique to determine these tensile properties for each sample group. However, due to the limitation in the lab the grip width specified by the ASTM standard test method was reduced from 8 inches to 3 inches because the maximum jaw width available in the lab was 3 inches.

In the tension creep test, a sample (5 inches wide and 10 inches long) were mounted on an Instron (Figure 2.2 & 2.3) with a soft strip of brown cork layered between the glass yarns and the jaws to protect the glass yarns from being crushed (not necessary for the original sample). The cork material was marked on the edges between the jaws and testing fabric sample and was monitored to ensure no slippage between the fabric, cork, and the jaws. The jaws were 2 inches in depth and 3 inches wide and the gauge length was 6 inches. Thus, after clamping, the top 2 inches and bottom 2 inches at the center of the width are fully gripped by the jaws with inch extra width on both sides to prevent fraying of the yarns during the test. In both reinforcement methods, the 6 threads of glass yarns are fixed in the 3 inches center width and will contribute to the resistance of the elongation, IED and creep.

A cork liner is not used during the tension creep tests for original unreinforced samples due to the reason that no glass yarns need to be protected. Comparative tension creep tests using and without using cork liner on unreinforced samples cut from the same yarn sets (same weft yarns) were conducted at 1000N and 500N loading conditions along the weft direction. Results (See appendix B for statistical analysis of testing results) showed testing without cork liner is a more conservative approach since under 500N, the average total elongation of unreinforced samples tested with cork liner was higher than the average total elongation of unreinforced samples tested without cork liner. A lower average elongation from original unreinforced

samples will likely results in an average lower elongation reduction when compared with elongation results from reinforced samples.

Before the experiment starts, tensile properties of the substrate and the glass yarn used were tested. Two parameters needed to setup an appropriate creep tensile test procedure were also determined. These parameters are: 1. the designed holding load, and 2, the designed holding time. They each represents the designed load capacity and service time for the reinforced PE fabric product.

2.3.1 Determining tensile properties for original PE fabric

To determine the tensile properties of original PE fabric, five of the original PE fabric specimens were subjected to a load at machine speed of 300mm/min until the specimens broke. This was necessary to determine the maximum tensile capacity of the unreinforced fabric. The load – extension curve is given in Figure 2.4, and the maximum breaking load, extension at break, maximum strain, instantaneous elastic deformation (IED), IED at zero slope and load at IED are given in Table 2.2.

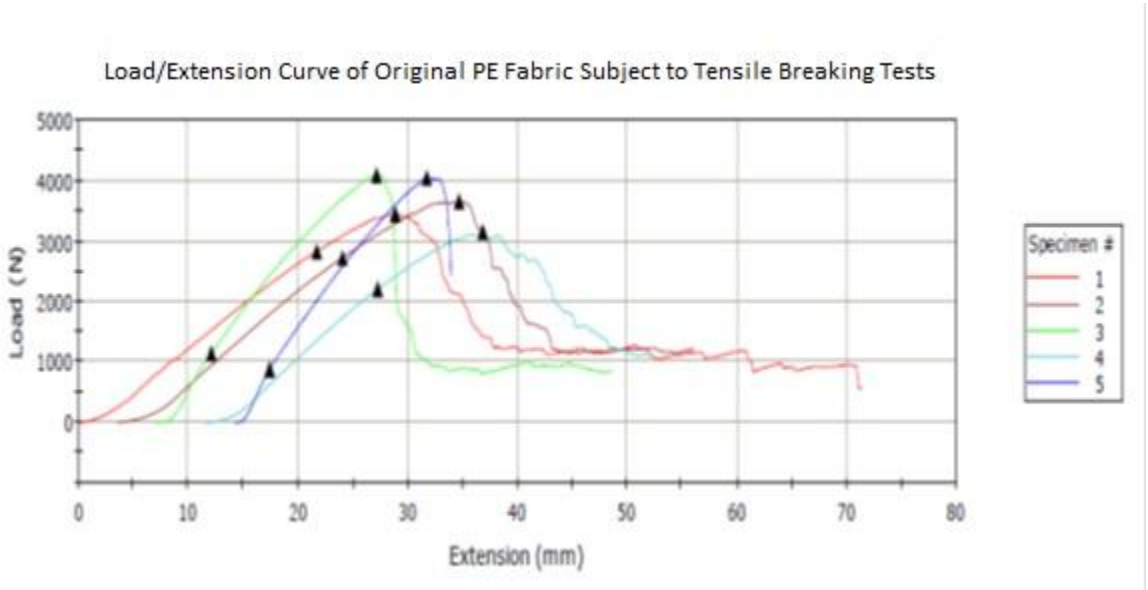

Figure 2.4. Load -Extension curve of original PE fabric and maximum breaking load.

Table 2.2. Tensile properties for original (unreinforced) PE fabric (From Figure 2.4).

Specimen No.	Maximum load (N)	Extension at Max Load (mm)	Maximum Strain (%)	IED at zero slope (mm)	Load At IED (N)
1	3444.52	28.88	19.25%	28.88	3444.52
2	3656.35	31.12	20.75%	31.12	3656.35
3	4087.45	20.03	13.35%	20.03	4087.45
4	3150.56	26.12	17.41%	26.12	3150.56
5	4046.63	17.46	11.64%	17.46	4046.63
Ave.	3677.10	26.54	16.48%	26.54	3677.10
SD.	398.97	5.81	3.19%	5.81	398.97

2.3.2 Determining tensile properties of glass yarn

In these tests, 10 specimens of 320tex glass yarns were tested for maximum load and extension using ASTM D2256-10. Results of load /extension curve and numerical values including maximum load, maximum extension, and IED are illustrated in Figure 2.5 and given in Table 2.3.

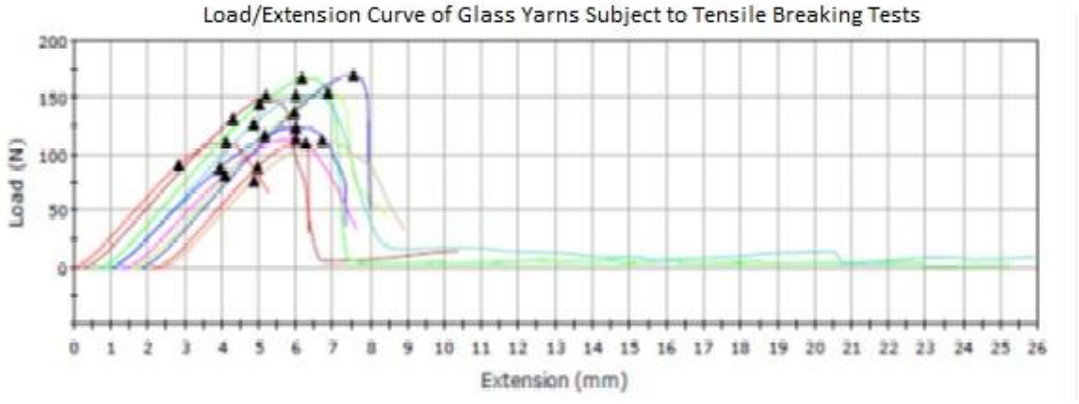

Figure 2.5. Load / Extension curve of glass yarn's maximum breaking load tests.

Table 2.3. Breaking test results of 320 Tex glass yarns (From Figure 2.5).

	Maximum load (N)	Extension at Max Load (mm)	IED (mm)
1	110.92	4.12	4.12
2	151.86	4.92	4.92
3	167.84	5.63	5.63
4	152.24	5.20	5.20
5	123.91	4.94	4.94
6	113.9	4.68	4.68
7	154.63	5.28	5.28
8	170.18	5.70	5.70
9	110.12	4.16	4.16
10	112.27	4.33	4.33
Ave.	136.79	4.90	4.90
SD.	±22.563	±0.46	±0.46

2.3.3 Establishing time for creep tests

After the test starts, the jaws exert tension force on the specimens and cause them to elongate. About 1000 seconds later, the creep rates of all 3 groups of specimens stabilized to a much slower rate and tended to continue to elongate at stable rates as shown in Figures 2.6 and 2.7. Thus, the test time of creep behavior for this current study has been set for 3600 seconds (one hour), which is long enough to capture the characteristics of time dependent creep properties of specimens since the creep rates became stabilized and predictable after 1000 seconds.

2.3.4 Establishing holding loads for creep test

The breaking load of the original fabric and glass yarn were measured to determine the holding loads for the tension-creep test. The breaking load of the original fabric and glass yarns are given in Tables 2.2 and 2.3.

It can be seen from Table 2.2 that the average maximum load an original PE fabric can sustain before breaking is 3677N. The breaking load of the original fabric was used to establish

the appropriate holding load which is the constant load of tension applied to the specimens for the time-dependent tension creep test on both the original PE fabric and reinforced fabrics. For this purpose, a series of holding loads starting from 2000N, 1500N, 1000N and 500N were applied for one hour. It was found that there were no significant differences of creep at 2000N and 1500N loading conditions for both the samples of the original group and the reinforced groups. More importantly, glass yarns in reinforced specimens broke quickly under 2000N and 1500 N loading conditions in the first 30 seconds and were clearly not strong enough to sustain the tensile loads at these two levels. When the loading condition was reduced to 1000N, the glass yarns on Group L-1000 specimens were able to sustain the load for one hour without breaking. However, the stitched specimens (Group S-1000) continued to break during tests. Until the applied load was reduced to 500N, glass yarns in Group S-500 specimens were able to sustain the load for one hour without breaking. Therefore, 1000N and 500N loads were selected as the holding values using the preliminary test results to test creep behavior and other mechanical properties.

2.4 Preparation of cast

Casting fabric formworks using glass yarn reinforced fabric by stitching method was made in lab as shown in figure 2.6. The mold was designed to cast 6” by 6” (6 inches tall and 6 inches in diameter) concrete columns. One mold labeled A was made with the fabric with glass yarn facing inside of the mold and the other one was labeled B with the glass yarn facing outside (PET thread facing inside).

The wood scaffold for the formwork was made by an 8” by 8” (8 inches width and 8 inches length) square plywood base mounted with two standing stripes of plywood (4” by 6”) that clamps the fabric part (6” by 20”) to form a 6” by 6” column container for the cast as shown

in Figure 2.6. The fabric was stabled along the length of the clamping strips and on the each outside of the clamping face, the bottoms of the wood stripes were bolted by 3” nails drilled from 1” above down to the wood base at 45^{o} diagonal direction. On top, an iron clamp was applied to clamp the plywood clamp tighter (this can also be down by bolting the top together with a nail).

The concrete was mixed with water at ratio of 1.9 liters per 55 pounds of concrete and poured into the mold. The mold was removed in the next day after the concrete is cured.

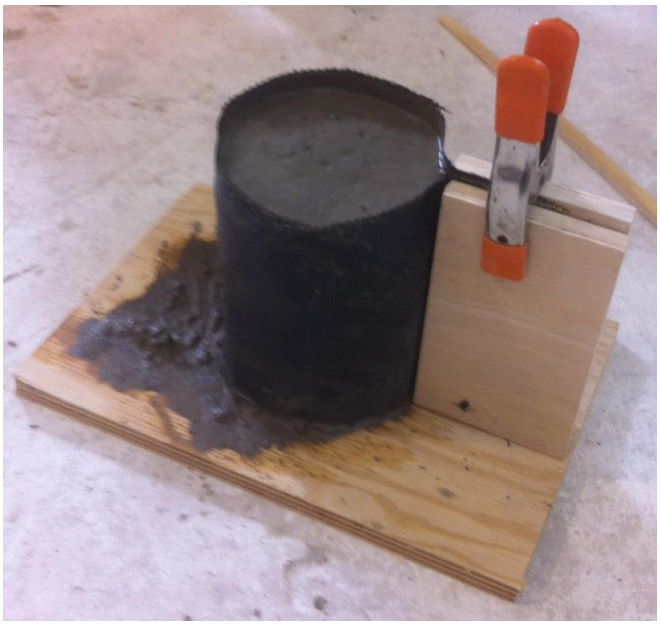

Figure 2.6. 6” by 6” concrete column is cast in fabric formwork made from wood scaffold and glass yarn reinforced fabric by stitching method.

Chapter 3. Preliminary studies using glass yarn reinforcement

3.1 Sample preparation

Two sets of preliminary tests were conducted to gain insight into the concept of reinforcement. At first test, two pieces of Geotex® 315ST fabric were "reinforced" with 4 threads of fiber glass yarns (obtained from the lab before the official glass yarn was requested, unknown maker) stitched at each end of the specimens to mimic a yarn that was woven into the fabric (Figure 3.1a), and were tested for tensile strength on the Instron 5965 using the grab method (ASTM D5034 - 09). The specimens with dimensions of 75mm width and 175mm long were clamped in two jaws 75mm apart and pulled at 300mm/min extension rate until 40% of the tensile drop was experienced on the machine. Peak strengths were recorded. However, creep tests were not able to conduct due to the fact that glass yarns break too early (first a few seconds) in the test.

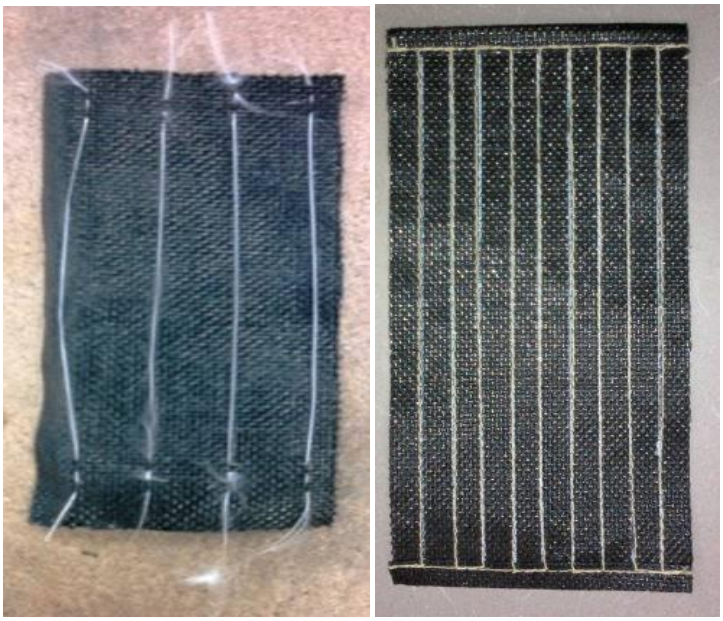

Figure 3.1. Pre-test samples. a) left, Geotex® 315ST reinforced with fiber glass threads by stitching at each ends and b) Geotex® 315ST reinforced by Kelvar stitches.

At the second test, five pieces of Geotex® 315ST fabric (150mm by 125mm) were reinforced by stitching across the fabrics with Kelvar threads at each half inch intervals (Figure 3.1b)[4]. The stitches were sewn in K9 Storm's factory. The stitching pattern was 301 stiches (ASTM D6193-11) at 6 stiches per inch with both Kelvar top thread and Kelvar bottom threads per inch interval across the width as shown in Figure 20. The samples were mounted onto the test instrument Instron 5965 and were stretched at a constant load of 2000 Newton (half the breaking load)[5] for 30 minutes then compared to the original Geotex® 315ST fabric which was also stretched under same load and time.

3.2 Discussion of the results

From the first test, the enforced fabrics had no higher strength than the non-enforced fabrics and creep result is unknown due to the broken glass yarn in the early stage of the creep tests. However, the glass yarn reinforced specimens showed a more uniform yarn breaking pattern than the unreinforced specimens. As show in Figure 3.2 unenforced fabric on the left had a concentrated breaking area at its center which was bulged after removal from the testing machine and the fabrics with glass fiber on the right were flat. The breakage was distributed evenly along the middle section which was initially pulled between the two jaws. Therefore, gave a positive indication that incorporating glass fiber yarns into Geotex® 315ST fabric it may improve its mechanical stability.

[4] At this point of time, kevlar is used as an alternative material for glass fiber due to their similarity in stiffness because the glass fiber thread is yet to be obtained for further experiments.
[5] This load is set higher than the safety load of a PE fabric which is usally 20% of its breaking strength because there will be no significant differences within 30min testing time if the load is under its safety load or it will take a very long time to show comparable results.

Figure 3.2. Breaking patterns of pre-test samples. Unenforced Geotex® 315ST (left), and fiber glass yarn enforced Geotex® 315ST (right).

The extension-time curves for the creep tests of original fabric and Kelvar reinforced PE fabric were graphed and calculated by Instron softwear Bluhill® 2.0 as shown in Figure 3.3a and 3.3b. The numerical results is shown in Table 3.1

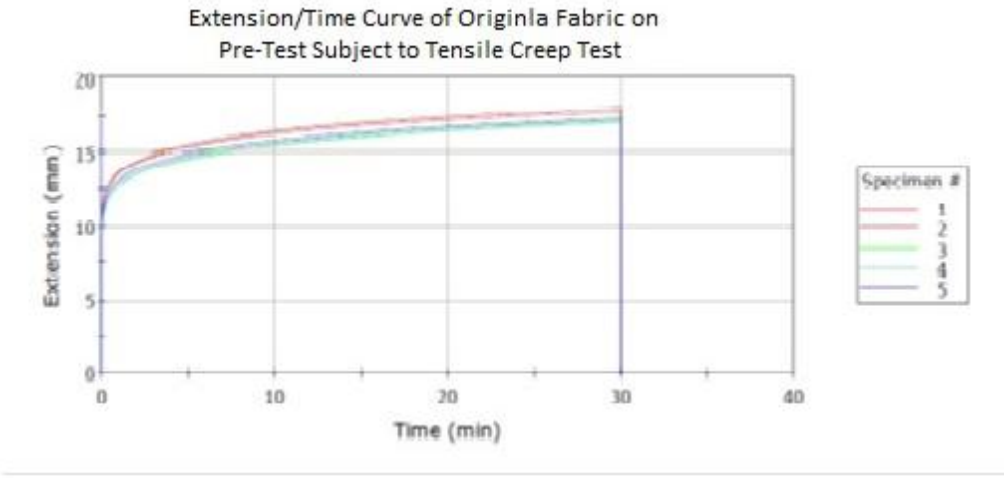

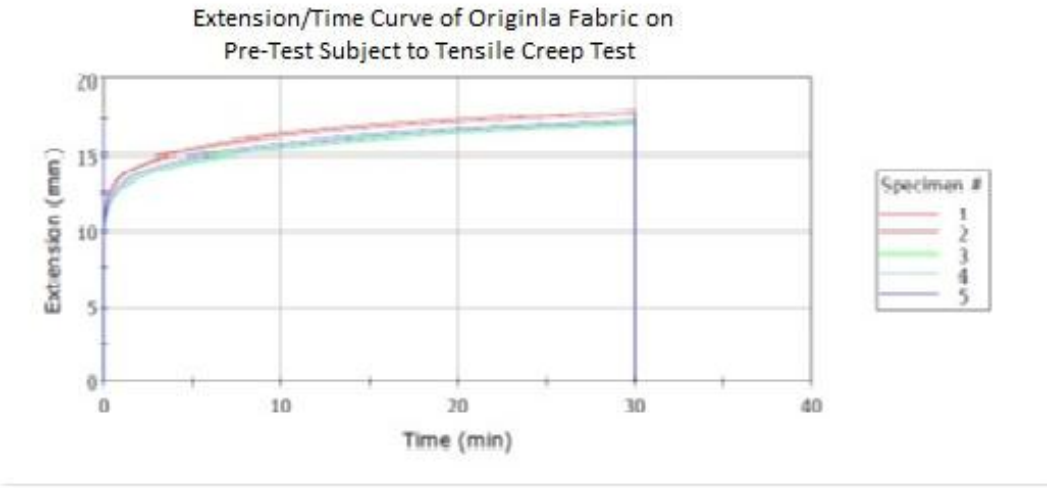

Figure 3.3. Test results of pre-test samples. a) top, extension overtime of original Geotex® 315ST fabrics. b) bottom, extension overtime of Kevlar stitching reinforced Geotex® 315ST fabrics.

Table 3.1 Average results of preliminary creep tests for Original Geotex® 315ST fabric and Kevlar Stitching Reinforced Fabric.

	Original Geotex® 315ST Fabric	Kevlar Stitching Reinforced Fabric
Average Total Extension (mm)	17.46	14.50
Average IED (mm)	12.50	11.00
Average Creep (mm)	5.00	3.5

From the results in Table 3.1 from the second test, the original samples had an average total extension at 17.5mm which about 12.5mm was IED, estimated from the curve in Figure 27a. The total creep of Kelvar reinforced specimen was at average 14.5mm with estimated IED around 11mm from Figure 27b. In 30min the stretch over time was nearly linear for both sample sets and Kevlar enforced samples showed lower time dependent stretch (creep: total stretch - instant stretch) at approximately 3.5mm. Compare to the original samples at 5mm, it was 1.5mm less. Because both creep behaviors were linear over time, we can predict that the difference in 1 hour of stretch would be 3mm. This reduction was significant if we consider the factor that the concrete starts to harden approximately after one hour and the fluid pressure starts to decrease[6]. Therefore, it can be concluded that the stitching method to imbed a low creep yarn have positive effect on reducing the time dependent creep as well as the instant stretch of Geotex® 315ST fabric.

[6] Actual rate of fluid pressure reduction in a mould depends on a complex of factors including" permeability of the mould wall, ambient temperature, mix design, pour rate.

Chapter 4. Effect of glass yarn reinforced PE composite on tensile properties

The official creep tests were conducted on the 6 groups of the specimen listed in Table 2.1. These specimens were subjected to 1000N or 500N holding load for an hour under ASTM D5262 – 07 and results are discussed in this chapter. The results of elongation, IED, modulus and creep of these groups were given in Table 4.1 and 4.2.

Statistical analysis is conducted using one tailed T test with unequal variance assuming the null hypothesis to be no difference among comparing groups.

Value of T is obtained by

$$t = \frac{\overline{X}_1 - \overline{X}_2}{s_{\overline{X}_1 - \overline{X}_2}} \quad \text{for which,} \quad s_{\overline{X}_1 - \overline{X}_2} = \sqrt{\frac{s_1^2}{n_1} + \frac{s_2^2}{n_2}}.$$

$\bar{X}$ is the average value of the sample group, S is the value of standard deviation and n is the number of tested samples, which in this experiment, is 5 for all groups. Degree of freedom m is calculated by $1/m = C^2/(n_1-1) + (1-C)^2/(n_2-1)$, which $C = (S_1^2/n_1) / (S_1^2/n1 + S_2^2/n_2)$.

The hypothesis is rejected if t value is greater than the value of $t_{m,\ 0.95}$ from the t-distribution table. $t_{m,\ 0.95}$ value is chosen from the table from the lowest m value calculated among groups to maximizing the value of $t_{m,\ 0.95}$ and increase the difficulty to reject null hypothesis.

Statistical analysis of results of elongation, IED, modulus and creep of these groups were given in appendix A and discussion of individual properties is presented in following sections.

4.1 Changes in elongation properties

The elongation, strain (%) and reduction in strain (%) of Group O-1000, L-1000, S-1000, O-500, L-500, and S-500 samples are given in Tables 4.1 and 4.2. It can be seen from these two

tables that Group O-1000 and O-500 samples (original PE textile) showed the largest average elongation after one hour compared to the reinforced specimens that were under the same loading conditions. The total elongation for Group O-1000 and O-500 was 14.13 mm and 8.74 mm respectively. Comparing the two groups of specimens with glass yarn reinforcement, the Group L-1000 specimens (glass yarn laminated PE) had 11.41 mm elongation which was lower than Group S-1000 specimens (glass yarn reinforcement PE by stitching method) which had 12.85 mm elongation. It can be seen from Table 4.1 that Group L-1000 specimens reduced elongation by 2.72mm, which was a 19.25% strain reduction from Group O-1000. Group S-1000 reduced elongation by 1.28mm, which was a 9.06% strain reduction from Group O-1000. The reduction on total elongation was more in Group L specimens than Group S specimens in this loading condition. However, under statistical analysis (appendix A), the differences between groups under 1000N loading condition were not significant.

Under 500N loading condition (Table 4.2), the reduction in elongation and strain (%) were 5.09 mm and 41.76% respectively for Group L-500 samples; and 3.65 mm and 67.41% for Group S-500 samples. It seems that the impact of reinforcement was much more significant under the 500 N loading condition than under the 1000 N loading condition. Further, Group S-500 samples showed larger reduction in elongation and strain (%) than Group L-500 specimens. Under the 500N loading condition, the glass yarns in Group S-500 specimens were locked in position at every stitch by the polyester top thread and had no freedom to slip; the glass yarns can hold the base fabric from stretching better than the glass yarns in Group L-500. Thus, Group S-500 had more elongation reduction at 5.90mm compared to Group L at 3.65mm. The statistical tests comparing the means of elongations among 3 groups (appendix A) showed that group L-

500 had significant lower elongation than group O-500, group S-500 had significantly lower elongation than both group O-500 and L-500.

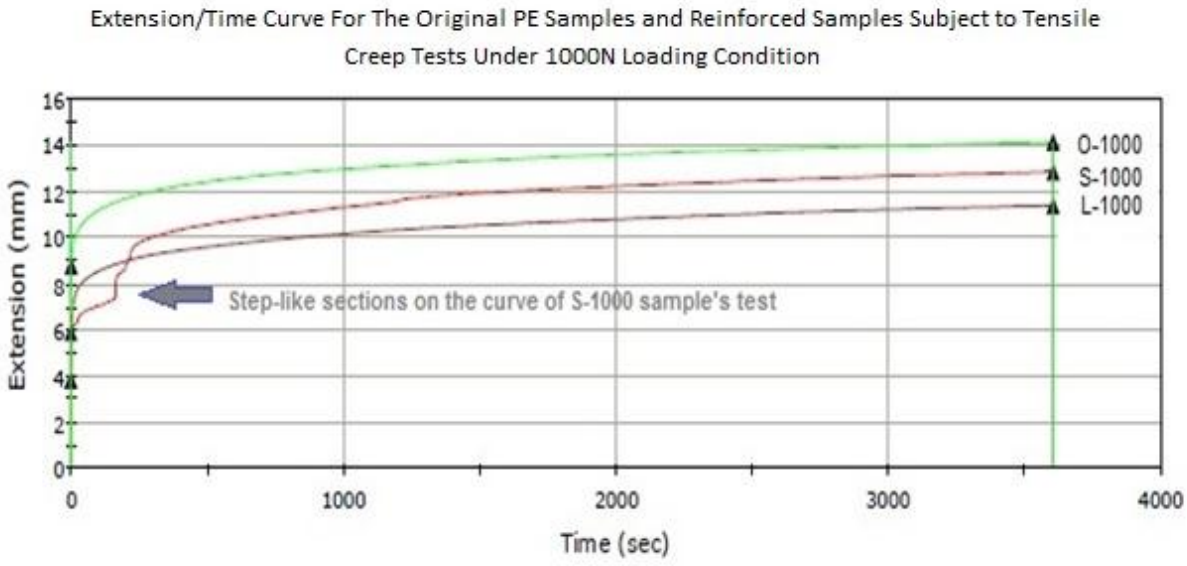

Figure 4.1. Extension-Time curve under 1000N loading condition tests (curves are selected individual tests which show median results of total elongation in the group to avoid having many curves showing on one graph).

Table 4.1. Changes in mechanical properties under 1000 N loading condition after 1 hour.

Group	Elongation (mm)	Total Elongation Reduction (mm)	Total Strain	% of reduction strain	Initial modulus (MPa)	IED at zero slope (mm)	Creep (mm)
O-1000	14.13 ± 3.64	0	9.42%	0.00	586.85 ± 4.27	8.67 ± 0.34	5.46 ± 3.99
L-1000	11.41 ± 2.94	2.72	7.61%	19.25%	1263.52 ± 9.18	3.85 ± 0.15	7.56 ± 3.10
S-1000	12.85 ± 3.31	1.28	8.57%	9.06%	903.03 ± 6.56	5.81 ± 0.23	7.04 ± 3.55

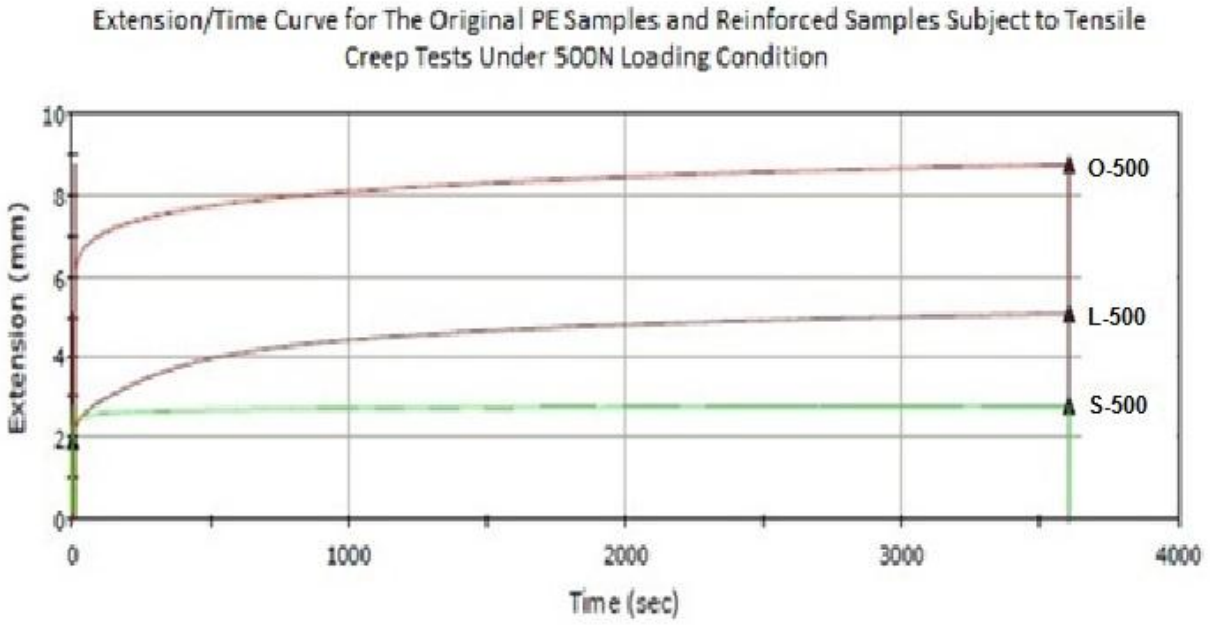

Figure 4.2. Strain/Time curve under 500N loading condition tests (curves are selected individual tests which show median results of total elongation in the group to avoid having many curves showing on one graph).

Table 4.2. Changes in mechanical properties under 500 N loading condition after 1 hour.

Group	Elongation (mm)	Total Elongation Reduction (mm)	Total Strain	% of reduction strain	Initial modulus (MPa)	IED at zero slope (mm)	Creep (mm)
O-500	8.74 ± 2.34	0	5.83%	0.0	532.47 ± 4.77	5.98 ± 0.22	2.76 ± 2.11
L-500	5.09 ± 1.91	3.65	3.39%	41.76%	1121.04 ± 5.97	1.98 ± 0.11	3.11 ± 2.02
S-500	2.84 ± 1.23	5.9	1.89%	67.51%	898.24 ± 3.26	2.31 ± 0.15	0.53 ± 1.05

During the tension creep test under 1000N loading conditions, it was observed that glass yarns in Group S-1000 specimens were not able to sustain the tension and eventually broke (Figure 4.1). Although they all broke within 500s (seconds) from the start of the test, some broke suddenly and some broke more slowly. The breaking processes of glass yarns were observed and can be seen from Figure 4.1: There are a few steps-like segments at the beginning (left side) of

the Time vs. Elongation curve of the S-500 specimen. These step-like segments were caused by the sudden break of some glass yarns in the reinforced specimen. Each sudden break released some elongation instantly when the resistance to stretch provided by the glass yarns was diminished and shifted the curve upwards. No such phenomenon was noticed for Group O-1000 and L-1000 samples as well as in all three samples under the 500 N loading condition.

The Group L-1000 specimen showed a smooth curved elongation-time relationship (Figure 4.1) and the elongation was always lower than Group O-1000 and Group S-1000. This is because the glass yarns were better able to sustain the 1000 N load and limit the fabric from stretching. Compared to the breaking test results for glass yarns (Table 2.3), the total elongation of Group L-1000 specimens (11.41 mm: Table 4.1) was much higher than the maximum elongation of the glass yarns themselves (4.9 mm). The maximum load that 6 glass yarns can sustain is approximately 800N as average breaking load for one glass yarn is around 136N, six of them together (six glass yarns were laminated) is thus 816N. When pulled by the 1000N load, the PE base fabric was much less stiffer than the glass yarns, all tension was primarily exerted on the glass yarns and they should have broken at their maximum capacity of 800N or their breaking elongation around 5mm (Table 2.3). However, glass yarns laminated on Group L-1000 specimens survived the tension all the way through the course of the test and reached an elongation of 11.41mm which is more than twice its maximum elongation. This indicates the likelihood that the glass yarns were slipping under the laminated coating to accommodate the stress and thus avoid being broken. Visual inspection of the laminated samples after testing revealed the formation of crimps by the glass yarns under the coating as shown in Figure 4.3. When applied stress is higher than the combined strength of reinforced yarns, laminated glass

yarns can slip without breaking. A similar crimp was developed under 500 N loading condition for L-500 samples, but the severity was much less.

Thus, from the results of the total elongation under 1000N and 500N loading conditions, we can conclude that the advantage of a textile reinforced by glass yarns under lamination is when it is subject to an unpredictably high load or even impacts, it can avoid breakage and dramatic failure. The disadvantage of such a textile is that it has less creep resistance than the glass yarn reinforced textile by stitching method. The advantage of the glass yarn reinforced textile by stitching method is that if the loading condition is within the glass yarn's capability the reinforcement provides much better creep resistance than the laminated textiles but when the load is higher than the glass yarn's maximum strength, they may break suddenly and cause dramatic failure.

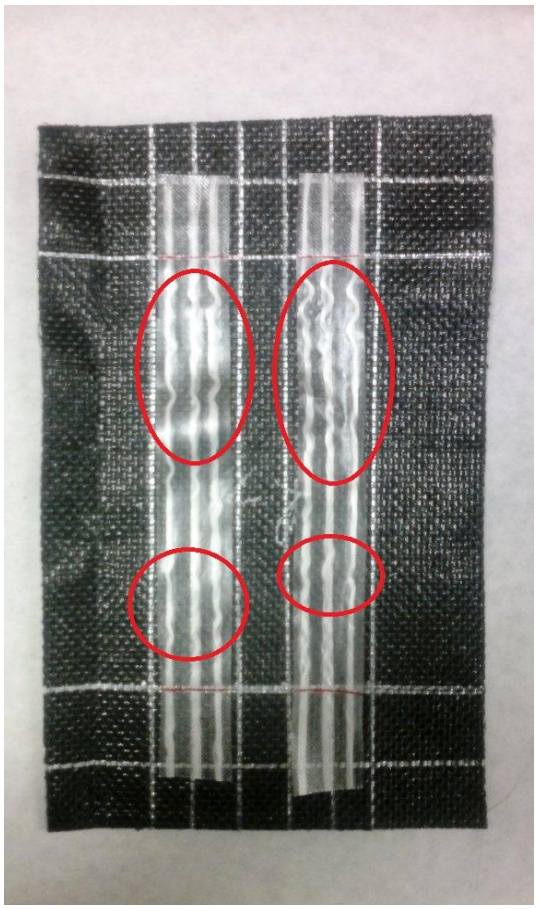

Figure 4.3. Glass yarns are crimped during the test under 1000 N loading condition (Crimping is marked by the red circles).

4.2 Instantaneous elastic deformation (IED)

The elongation point where the PE fabric reaches its maximum elastic stretch without undergoing plastic deformation (creep) is the extension at yield (the zero slope moment on the extension versus time curve, Figure 4.4). The amount of elongation or extension from start to the yielding point is referred as Instantaneous Elastic Deformation (IED). The IED data of all 6 groups of specimens were obtained from the values of their yielding point as zero slope and are given in Table 4.3. It can be seen that Group O-1000 and O-500 specimens produced the highest IEDs when compared to other groups under the same loading conditions (1000N: 8.67mm; 500N: 5.98mm) and Group L-1000 and L-500 had the lowest IEDs under both loading

conditions (1000N: 3.85mm and 500N: 1.98mm). Group S-1000 and S-500 had medium IED values (1000N: 5.81mm and 500N:2.31mm). Under statistical analysis (appendix A), the differences between groups were significant.

At the yielding point of elongation, the pulling (top) jaws from the Instron tester would experience a sudden increase of resistance from the specimens as the elasticity was exhausted and the computer would record a near zero slope point on the extension-time curve (Figure 4.4). In the tension creep tests under 1000N and 500N loading conditions, the average yielding elongations of 5 tested specimens from each group and their loads at the yielding points are given in Table 4.3. The results are the average value of 5 specimens from each group. Also, the average values of elongations when the initial slope (the maximum slope indicated as 100% slope in the graph in Figure 4.4) dropped to its 80%, 60% and 40% values were also given. These values are necessary to determine the IEDs when the moment of zero slopes (100% drop) cannot be detected from some of the test specimens. Figure 4.4 provides the graphic illustration of the IED and yielding point at zero slope thresholds, 80% slope threshold, 60% slope threshold and 40% slope threshold. The undetected zero-slope will be discussed in the subsequent section.

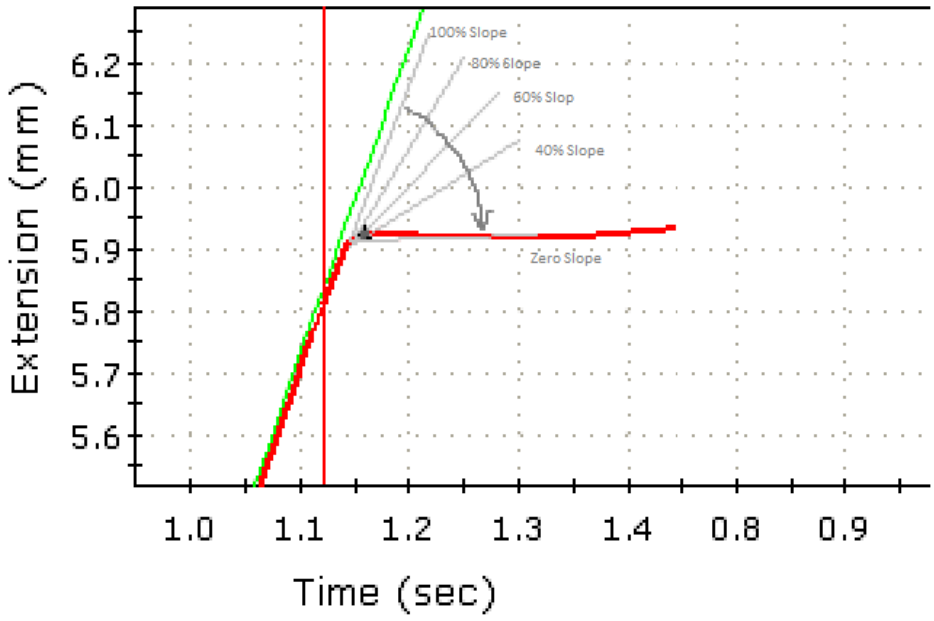

Figure 4.4. Magnified curve section at the yielding point from curve of Group L specimen. The black triangle mark indicates the yielding point at the zero slope which is a 100% slope drop from the initial slope. Added grey line indicating the initial slope moment (100% slope), 80% threshold slope moment, 60% threshold slope moment, 40% threshold slope moment and zero slope moment.

Table 4.3. Yielding elongation at zero slope, 80% maximum slope, 60% maximum slope and 40% maximum slope and load at the yielding points.

Groups	IED (mm)	Extension at Yield (mm) (Zero Slope)	Load at Yield (N)	Extension at Yield (mm) (Slope Threshold 80 %)	Extension at Yield (mm) (Slope Threshold 60 %)	Extension at Yield (mm) (Slope Threshold 40 %)
O-1000	8.67	8.78	1026.11	8.71	8.71	8.8
L-1000	3.85	3.85	1041.29	3.86	3.96	3.96
S-1000	5.81	5.93	1026.67	2.97	2.97	2.97
O-500	5.98	5.98	499.97	5.97	5.97	6.06
L-500	1.98	Some value not detected	500.77	0.61	1.98	1.98
S-500	2.31	Some value not detected	501.16	0.72	2.31	2.31

When the zero slope moment is not detected by the Instron Tester due to the plastic nature of the fibre, an observation from the elongation from the points at yielding of 80%, 60% and 40% of the slope threshold (Table 4.3) is needed to estimate the IED. The examination of the results in Table 4.3 from 80%, 60% and 40% of slope thresholds could reveal at what elongation

the slope had dropped dramatically and thus the IED can be approximated from that elongation. For example, some test specimens from Group S-500 samples had no zero slope point detected and thus the average yielding elongation at the zero slopes cannot be calculated. However the average elongation of 80% slope threshold (20% drop of slope) was at 0.72mm, 60% was (40% drop of slope) at 2.31mm and 40% (60% drop of slope) was at 2.31mm (Table 4.3). It can be stated that since the rate of stretch is largely decreasing from 60% slope threshold to 40% slope at 2.31mm elongation (Slope Threshold 60% and 40%), the resistance to stretch is dramatically increasing at 2.31mm elongation and the approximate yielding point or IED is at 2.31mm elongation for this zero-slope undetected S-500 specimens.

However, from Table 4.3 it can be noticed that the load experienced at the yielding elongation is close to the tests' pre-set maximum holding loads (1000N and 500N). This means that the zero slope is more likely caused by the stopping of the jaws when the pre-set holding loads were reached rather than the sudden increase of the resistance from the specimens when their initial elasticity is exhausted. In fact, the PE original fabric is a plastic material, thus the boundary between elastic deformation and creep does not exist. Cheng, Polak, & Penlidis's paper suggested that elastic and plastic deformation happens simultaneously for PE fabrics under stress (Cheng, Polak, & Penlidis, 2011). Thus the IED obtained in the present study from the breaking test (Table 2.2) and creep-tension tests (Tables 4.1 and 4.2) was not strictly elastic deformation, but contained some initial creep. Nevertheless, these values reflect the immediate response of the specimens when tensile force was applied.

4.3 Initial modulus

The initial modulus results (young's modulus) are given in Tables 4.1 and 4.2 for all 6 groups of samples. It can be seen that the Group O-1000 and O-500 samples produced the lowest

average modulus of 586.85 MPa and 532.47 MPa respectively; Group L-1000 and L-500 specimens produced the highest modulus at 1265.50MPa and 1121.40MPa respectively; and Group S-1000 and S-500 is in the middle at 903.0 MPa for 1000N and 898.2 MPa for 500N loading conditions. These results suggest that reinforcement by stitching (Group S-1000 and S-500) and by lamination (Group L-1000 and L-500) increase the modulus of the specimens. Moreover, modulus increases in the laminated specimens were more than double than that of the original PE fabric and the modulus increase in stitch reinforced specimens was about 50% more than the original (Tables 4.1 and Table 4.2). Under statistical analysis (appendix A), the differences between groups were significant.

The initial moduli reflect the IED measurements that a lower IED is associated with a higher modulus. Initial modulus (Young's modulus) is the modulus of the specimens at the beginning of the stretching within the IED. Ideally, the IED and initial modulus measures the specimen's elastic resistance within their elastic regions but in woven textile specimens such as the ones used in this research, the crimp within inter-woven yarns would cause the IED to be higher when the yarns were flattened under stress. The Group S-500 specimens produced the average total elongation of 2.84 mm which is lower than the Group L-500 specimens (5.09 mm, Table 4.2). The Group S-500 specimens are thus stiffer than the Group L-500 specimens. Although, the modulus of Group L-500 specimens was 1121.04 MPa which is higher than Group S-500 (898.24 MPa) indicating Group L-500 is stiffer than S-500.

The contradiction between the relationship of total elongation and initial modulus for group L-500 and S-500 specimens can be explained by considering the configuration of glass yarns in each reinforced specimen. The glass yarns in Group L-500 specimens were pulled straight, laid flat and laminated while in Group S-500, the glass yarns were not laid as straight as

in the lamination method because the during the stitching process, the top polyester thread grabs the glass yarn from the bottom bobbin while it was naturally hanging (Figure 2.3). When glass yarns were sewed onto the PE base fabric there was some crimp introduced to each stitching. Thus at the beginning of the test, the S-500 specimens had more to elongate than group L-500 specimens which resulted in a lower modulus and higher IEDs. During the tests, because the stitched glass yarns in S-500 specimens were more rigidly bound to the PE base fabrics than the glass yarns in L-500 specimens (which can slip under the coating), as soon as the crimps in S-500 specimens were straightened, the specimens became stiffer than Group L-500 specimens which limited the growth of the creep (which is discussed in the later section) during the rest of the test and eventually resulted in a lower total elongation for S-500 specimens.

The comparison of total elongation, initial modulus and IEDs for group L-1000 and S-1000 is not discussed because the glass yarns in S-1000 specimens were broken during testing.

4.4 Changes in creep property

The creep result for the three Groups of specimens under 1000N loading conditions and under 500N loading conditions are given in Tables 4.1 and 4.2 respectively. It can be seen from these tables that Group L-1000 and L-500 specimens produced the highest creep values of 7.56mm and 3.11mm respectively. Group O-1000 and O-500 specimens produced an average creep of 5.46mm and 2.76mm and Group S-1000 and S-500 generated 7.04mm and 0.54mm respectively. In 500N loading condition, the S-500 specimens showed more than 80% reduction in creep compared to Group O-500 specimens; while under the 1000 N loading condition the creep of Group S-1000 were 30% higher than Group O-1000. On the other hand, for Group L-1000 and L-500 specimens, the increased creep value was 40% and 13% higher than the Group O-1000 and O-500 specimens respectively. Under statistical analysis (appendix A), the

differences between groups were not significant for all groups under 1000N loading condition mainly due to yarn slippage in laminated sample and yarn breakage among stitch reinforced sample. There is also not statistical significance among L-500 and O-500 also due to the yarn slippage. The significance is found between S-500 and O-500 and S-500 and L-500 (note for this research prime and sec creep were not measure because they were not relevant for fabric formwork as once the concrete is harden it does not shrink back).

When the specimens under stress enter a stable creeping zone after the yielding transition (the large bending of the curves in Figures 4.1 and 4.2), the time and extension curve establish a near linear relationship. To analyze this relationship mathematically, the data points of time and elongation values along this curve were extracted at 1000s, 2000s, 3000s, and the end of the test at 3600s for both load conditions. Tables 4.4 and 4.5 show these data points for 1000N and 500 N loading conditions. Graph analysis of these date are illustrated in Figures 4.5 and 4.6. In order to obtain the creep rates (time dependent creep) for each loading condition, three linear equations from elongation – time curves for both loading conditions were calculated as shown below:

Equations for 1000 N loading condition (Y: creep in mm and X: time in seconds):

$Y = 0.0004x + 12.607$ ----- equation 1 (specimen Group O-1000);

($R^2 = 0.97$)

$Y = 0.0005x + 9.7712$ ----- equation 2 (specimen Group L-1000);

($R^2 = 0.98$)

$Y = 0.0006x + 10.886$ ----- equation 3 (specimen Group S-1000)

($R^2 = 0.95$)

Equations for 500 N loading conditions (Y: creep in mm and X: time in seconds):

$Y = 0.0003x + 7.8565$ ----- equation 1 (specimen Group O-500);

($R^2 = 0.97$)

$Y = 0.0003x + 4.2313$ ----- equation 2 (specimen Group L-500);

($R^2 = 0.96$)

$Y = 0.00003x + 2.7488$ ----- equation 3 (specimen Group S-500)

($R^2 = 0.96$)

The numerical constant number at the end of each equation theoretically represents the interception of the Y value when X = 0 but since the data is obtained after 1000 seconds and the XY relationships before 1000s were not linear, these numbers are not useful and thus will be ignored in the analysis.

Table 4.4. Elongation points extracted from 1000s, 2000s, 3000s, and 3600s under 1000N loading condition.

Sample Groups	IED (mm)	Holding Time (second)							
		1000		2000		3000		3600	
		Elongation (mm)	Creep (mm)	Elongation (mm)	Creep (mm)	Elongation (mm)	Creep (mm)	Elongation (mm)	Creep (mm)
O-1000	8.67	12.97	4.3	13.61	4.94	13.97	9.03	14.13	5.46
L-1000	3.85	10.18	6.33	10.81	6.96	11.24	4.28	11.41	7.56
S-1000	5.81	11.33	5.52	12.24	6.43	12.67	6.24	12.85	7.04

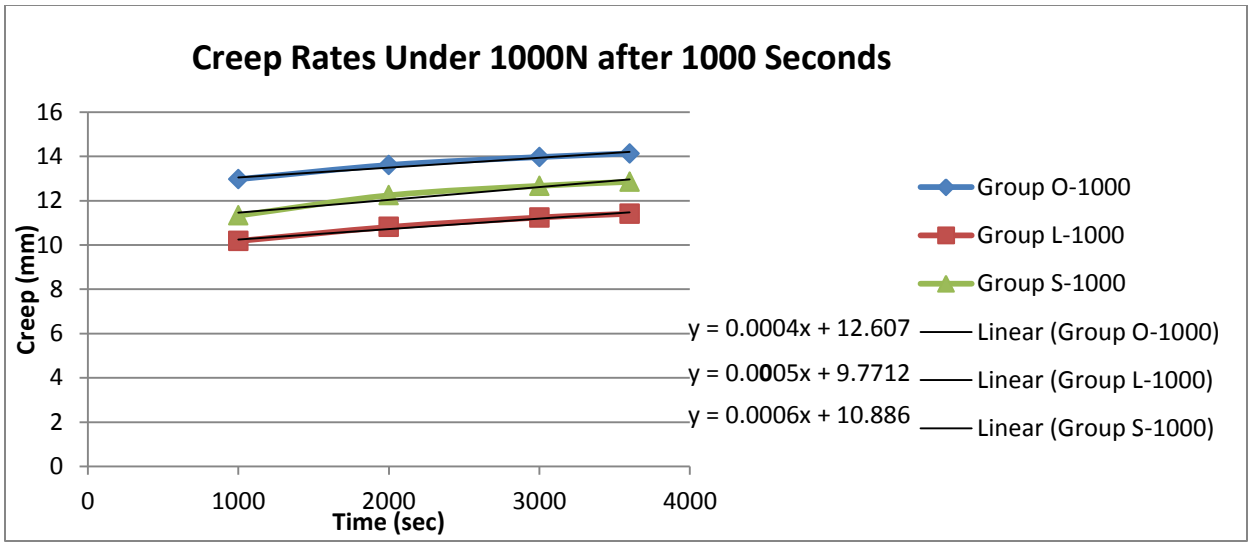

Figure 4.5. Graphic analyze of the creep behavior of 3 groups of specimen under 1000N.

Table 4.5. Elongation points extracted from 1000s, 2000s, 3000s, and 3600s under 500N loading condition.

Groups	IED (mm)	Holding Time (s)							
		1000		2000		3000		3600	
		Elongation (mm)	Creep (mm)	Elongation (mm)	Creep (mm)	Elongation (mm)	Creep (mm)	Elongation (mm)	Creep (mm)
O-500	5.98	8.07	2.09	8.43	2.45	8.64	2.66	8.74	2.76
L-500	1.98	4.43	2.45	4.81	2.83	5	3.02	5.09	3.11
S-500	2.31	2.77	0.46	2.81	0.5	2.83	0.52	2.84	0.53

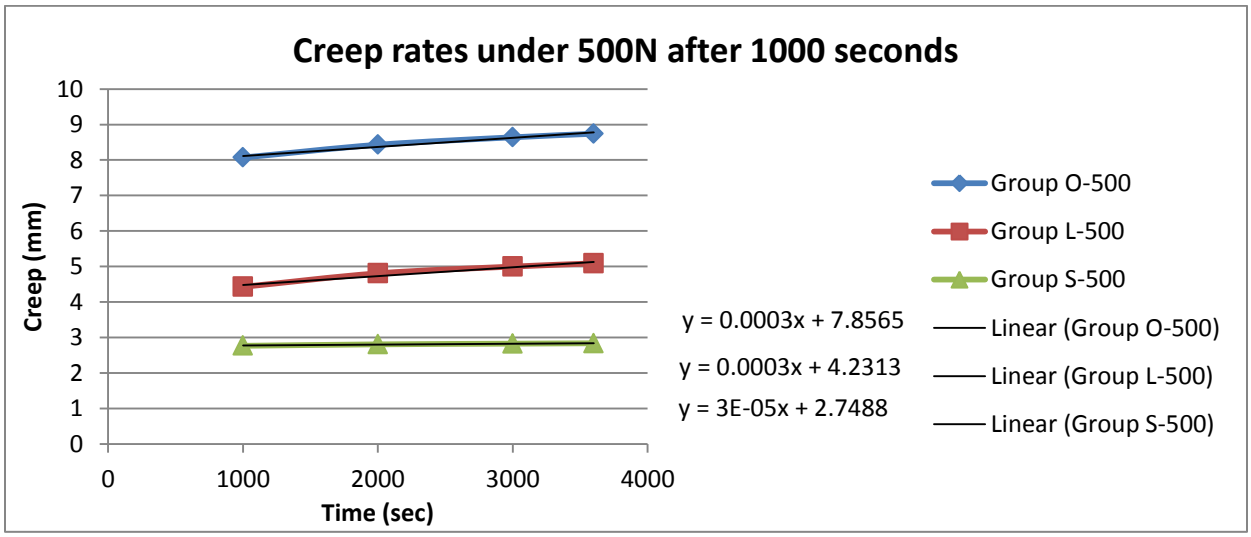

Figure 4.6. Graphic analyze of the creep behavior of 3 groups of specimen under 500N.

Under the 1000N loading condition, the creep rates between 1000s and 3600s are: 0.0004mm/s (4E-4 mm/s) for Group O-1000, 0.0005mm/s (5E-4 mm/s) for Group L-1000 and 0.0006mm/s (6E-4 mm/s) for Group S-1000. Under the 500N loading condition, the creep rates between 1000s and 3600s are: 0.0003mm/s (3E-4 mm/s) for Group O-500, 0.0003mm/s (3E-4 mm/s) for Group L-500 and 0.00003 mm/s (3E-5 mm/s) for Group S-500. The immediate conclusion is that under the 500N loading condition (S-500 specimens) the tendency to creep reduced significantly compared to the other two groups.

The creep rate for S-500 specimens under the 500N loading condition was only 3E-5 mm/s, 10 times slower than the rate of 3E-4 mm/s for Group O-500 and L-500 specimens. However, for Group S-1000 specimens, the creep rate was 20 times higher than the creep rate of Group S-500 loading condition when other two groups (O-1000 and L-1000) were only 33.33% and 66.66% higher respectively than groups O-500 and L-500.

The differential creep behaviors of glass yarn reinforced PE fabric by stitching method under two loading conditions can be explained by the fact that glass yarns broke under the 1000N loading condition. When the glass yarns were broken, all the stress was transferred to the base fabric and the resistance to stretch provided from the Group S-1000 specimens is no longer better than the Group O-1000 specimens. Additionally, before the glass yarns were broken, the Group S-1000 specimens had lower IED compared to Group O-1000 specimens (IED of Group O-1000: 8.67; IED of Group S-1000 specimens: 5.81; Table 4.1) and after the glass yarns were broken, the reduced IED that was held by the glass yarns is released to increase the creep. This resulted in the higher creeping rates for S-1000. Under the 500N loading condition, the glass yarns were able to hold the fabric all the way through the end of the test, and thus limit the creep to a very small amount.

Under both loading conditions, the Group L-1000 and L-500 specimens produced larger creep rates than the Group O-1000 and O-500 specimens. As discussed before, the glass yarns in Group L had some freedom to slip during the test. Since Group L-1000 and L-500 always have the lowest IEDs among the groups in the same loading conditions, the remaining unstretched portion of IED is released when the glass yarns start to slip. On the other hand, the specimens in Group O-1000 and O-500 always had the largest IEDs that exhausted a large portion of the total elongation and made the specimen more stable during the creep elongation than Group L-1000 and L-500. This observation of reduced creep rates due to larger IEDs can be made useful in some fabric formwork applications where if it is possible to stretch the fabric before using it may help to stabilize the fabric.

4.5 Comparison of non-mechanical advantages

These two methods of glass yarn reinforcement are proposed as solutions to an industrial problem. Compared to the reinforcement by lamination method the stitching method has possible advantages in cost efficiency:

1. The glass yarn fixing agent PET threads are much less expensive than vinyl coating.
2. The process of stitching is less labor intensive than process of lamination. The stitching process stiches the yarns directly onto the fabric while lamination process involves multiple steps including: lay down the glass yarns on the fabric and keep them straight (may also involves additional application of temporary glue to keep them straight and in place before heat bounded onto to the base fabric), apply coating materials to cover the glass yarn and then heat press.

3. The process of stitching is less problematic than the lamination process. The stitching machine runs flawlessly once the machine are setup but lamination methods have multiple non-continuous steps and are handled mainly by hand. Each step requires high level caution of the operator such as keeping the glass yarns straight or balance the pressing time of heat presser. The heat pressing step is especially difficult to control because the base fabric made from PE material is extremely heat sensitive. If applied slightly in excess the base fabric would shrink or melt, if applied less than required, the vinyl coating would not melt to bind the glass yarns and base fabric.
4. The glass yarn reinforced fabric through stitching method is much lighter than glass yarn reinforced fabric through lamination method because an extra layer of vinyl coating is heavier than a few lines of PET threads. Thus the transportation cost will be less for stitching reinforced fabric.
5. Due to extra layer of coating increases the thickness of the fabric and block the pores of the fabric, thus, other advantages of stitching reinforced fabric over lamination reinforced fabric include better drape and better permeability

Chapter 5. Surface characteristics of concrete column cast using stitching reinforced glass yarn PE fabric.

Two 6” high by 6” diameter concrete column specimens were cast in the fabric formwork made from the glass yarn reinforced PE fabric by stitching method. One formwork used the fabric as the glass yarn is faced inside mold A (Figure 5.1) and the other formwork used the fabric as the glass yarn is faced outside mold B (Figure 5.1). The results of surface character of the cast concrete and the used fabric is discussed in this chapter.

Figure 5.1 shows the surface of the concrete column from molds A –right side (glass yarn facing concrete, PET thread is outside) and B-left side (glass yarn facing outside, PET thread facing inside).

Figure 5.1. Cast result using stitching reinforced fabric. Column A (left top), is cast in the mold with galss yarns facing inside, collumn B (right top) is cast in mold with glass yarns facing outside. Left bottom picture shows the magnified vison the surface chracteristics collumn A and right bottom picture shows the magnified vison of the surface charicteristics of collumn B. Glass yarn caught on the concrete in collumn A is marked by a red circle.

From visual inspection, both columns A and B have horizontal impressions from the stitching lines from the fabric. However, column A's impression is much deeper, has a slight zigzag path, rougher surface around the grooves and have glass yarns caught inside the grooves. While column B's impression is more regular, nearly smooth with darker discoloration and no materials caught on the concrete.

The horizontal discoloration of column B as shown in Figure 5.1 is due to the slight rough surface caused by the irregularity of the formwork fabric along the stitching lines where PET threads ran through. Although the PET threads did not cause deep grooves or damages as those caused by the glass yarns, it made the surface slightly rougher than the rest of the surface. Thus, the light reflections of these rougher areas are more irregular and appear to be darker than those smoother areas. After showing them to Mark West, a highly experienced professor of architect, he commented that "Speaking on a purely architectural level, I think that the lines of stitching would make a much more beautiful column - essentially a "self-ornamenting"

formwork. I think this kind of formwork fabric would be aesthetically preferable to a 'normal' un-reinforced fabric (M. West, personal communication, July 10th, 2013).

The fabric from removed mold showed that glass yarns were broken completely from mold A when it faced inside while the fabric removed from mold B is nearly intact when the glass yarns were facing outside (Figure 5.2, circled in red). The glass yarn breakage occurred when glass yarns were caught in the concrete and pulled away during mold removal. Although in some places the glass yarns were completely broken as shown in figure 5.2, in many other places some of the filament yarns in the glass yarn were broken and were visible under a microscope (Figure 5.3). These partial breakages of filament yarns are illustrated in figure 5.3 in magnified pictures. There is no evidence suggesting glass yarns or filaments were broken before the mold was removed.

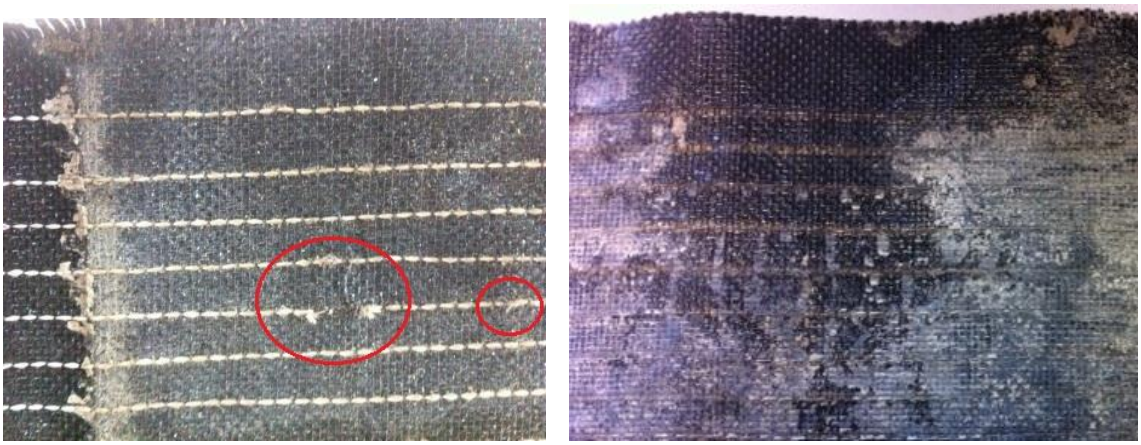

Figure 5.2. Fabric condition after cast. Fabric removed from mold A (left), is used with galss yarns facing inside; fabric removed from mold B (right) is used with glass yarns facing outside. Glass yarns are damaged during the mold removal process and are marked by red circles.

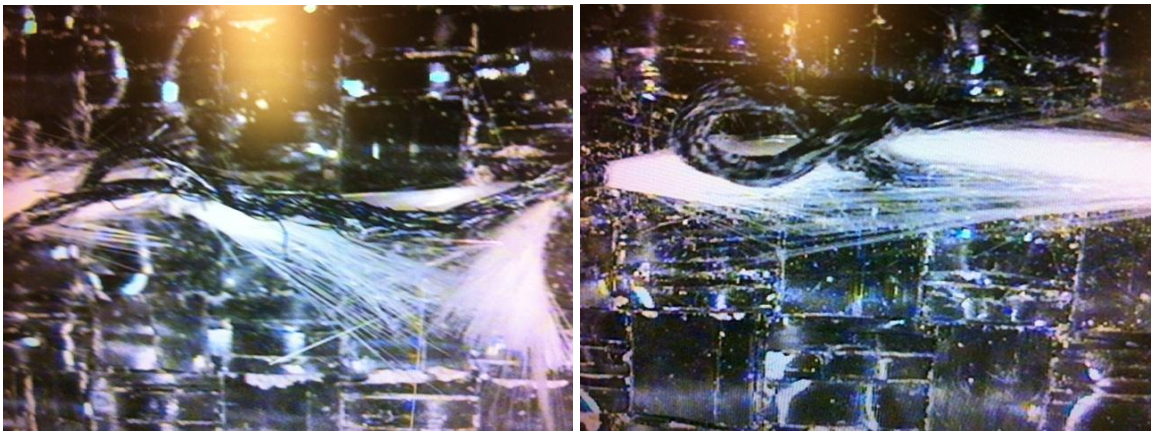

Figure 5.3. Glass yarn breakage (partially break) from mold A fabric.

Thus, above results showed that when glass yarns were faced inside, the uneven surface would damage the concrete surface and the concrete can also damage the glass yarn during the removal process and make it non-reusable. On the other hand, when glass yarns were faced outside and the less uneven side with PET threads was faced inside, the cast concrete had a much smoother surface with impressions that are considered aesthetic. The fabric mold is also undamaged and can be reused.

In addition to undamaged glass yarns, the reusability of the fabric formwork may also be affected by the concrete mix clotting the pores on the fabric and reducing its permeability – an important characteristic for fabric formwork. Figure 5.4 shows the fabric surface faced outside from mold B after removal from the cast column. The grey dusty deposits on the fabric (Figure 5.4 left) are fine cement mix particles bled through the pores of the fabric with water and cumulated around the pores when the water was dried. This may jeopardize the reusability of the fabric since the pores may be blocked by these deposits. After flushing with clean water most of the cement mix was removed (Figure 5.4 right) and the porosity of the cleaned fabric was compared to an unused fabric by examining the light passing conditions from the other side

(Figure 5.5). The comparison of these lights showed that the porosity of the used fabric after cleaning with water was no different from the unused fabric.

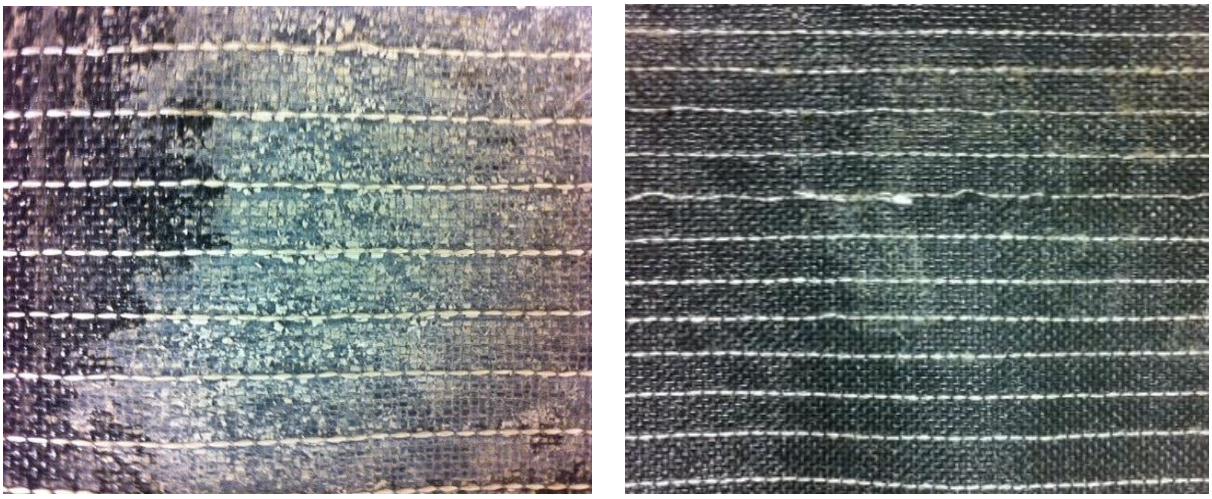

Figure 5.4. Fabric surface faced outside during casting from B: left – before cleaning and right – after flush with water.

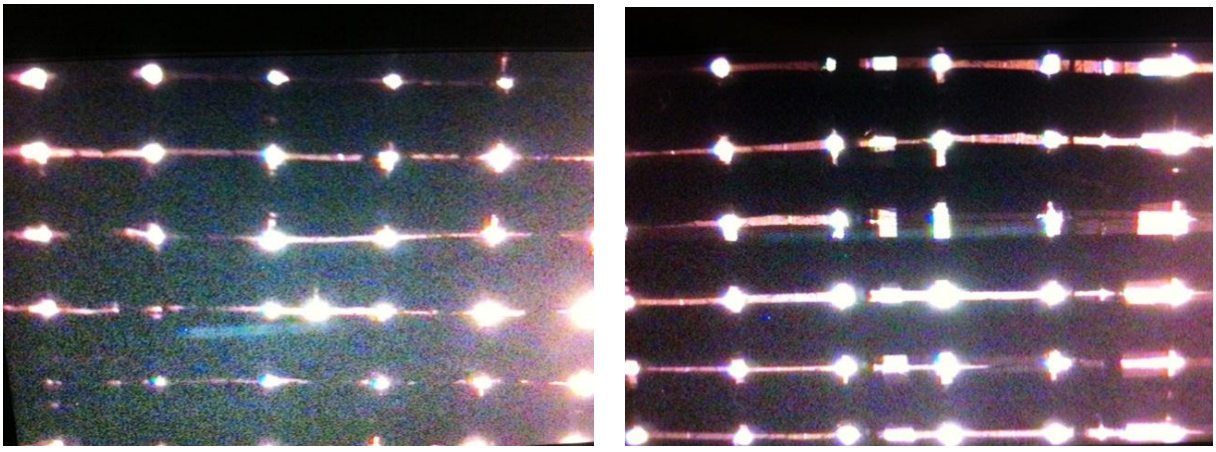

Figure 5.5. Light passage of wash cleaned fabric from B. When light were illuminated from the other side, the passing light showed the unused fabric (left) and used and cleaned fabric from mold B (right) have indifferent permeability.

The measured length in both molds after use is 20” and no noticeable dimensional change in other directions. However, these results need to be verified in future study by casting a full sized column that is approximately 3 meters tall because the 6” tall column in this experiment did not exert large enough pressure at the bottom of the fabric formwork that would cause the

fabric to deform or creep. Our conclusion that the fabric have reduced creep is based on the creep test conducted in chapter 4 which the 500N tensile force is applied and the initial modulus is close to 900 mega Pascal. If assume the glass yarns has a maximum strain at 0.4 (Miraftab, 2000.) without breaking, the maximum stress that the reinforced fabric can sustain is 900 MPa * 0.4 = 360 MPa. If also assume a safety factor of 2, the fabric is designed to take 180MPa stress. Introduce this tress at the bottom of the concrete assuming concrete's relative density is 2.4. and column height at 3 meters. The allowable column diameter within the designed capacity will be:

Concrete pressure is : relative weight to water is 2.40 × specific gravity of water 9806 N/m^3 × height 3 m = liquid pressure of fresh concrete at the bottom of height 3 m = 71Kpa.

Maximum hoop stress = 180MPa = 71KPa * R / t, which R is the column radius and t is the thickness of the fabric which is 0.2mm = 2 E-4 m.

R is obtained by solving this equation: R = 0.51 m => Diameter = 1.02 m = 39.92 inches.

Chapter 6. Conclusions and future work

The elongation property has been improved for both reinforced samples for all loading conditions in the increasing order of S-500>L-500>L-1000>S-1000. All reinforced samples showed an improvement in modulus for loading conditions. However, it was observed that the laminated samples produced the stiffer fabric due to the straight configuration of glass yarn in the composite fabric. As a result, the modulus of L-500 and L-1000 samples was much higher than the stitch reinforced samples. A significant reduction in IED was noticed for both reinforced samples for all loading conditions. The creep has been undesirably increased for both laminated samples and reinforced S-1000 samples due to the slippage and breakage of glass yarns; however, for the S-500 sample, a significant reduction in creep was obtained as the glass yarns' integrity was maintained. It is, therefore recommended that in order to reduce the time dependent creep during fabric formwork, the load should not exceed the maximum breaking load of all the reinforced glass yarns. Between these two reinforcement methods, lamination allows more creep but can resist breakage and rupture while the stitching method reduces creep more effectively as long as the loading condition is within the capacity of the glass yarns. In addition, glass yarn reinforced fabric through stitching method is more cost efficient, has better drape and better permeability than glass yarn reinforced fabric through lamination method.

When using glass yarn reinforced fabric for fabric formwork, the glass yarns perform better when facing outside of the mold. The slightly darker stitching line impression from the PET threads on the other side can be considered aesthetic.

The lab experiments have shown the glass yarn reinforcement by stitching method provides a solution for the dimensional instability of PE woven fabric when used in fabric formwork. Future study calls for in situ casting of objects with various sizes and shapes using

glass yarn stitched PE fabric to examine its suitability or shortages in different sites. For example, how big of a column can be cast in the formwork made from this fabric or how many reinforcement glass yarns are needed per inch space to hold the formwork for a 20ft high and 8" (or greater) diameter column?

In addition, when the glass yarn reinforced fabric was clamped at the joint of fixation as shown in Figure 2.6. The bending and the lateral compression at the joint may cause the glass to break easily. Thus, a study of how to avoid or reduce the degree of bending and compression on glass yarns in reinforced fabric at the fixation joint is also needed. In such situations that local breakages are hard to avoid. It is perhaps worth to investigate if the glass yarn reinforcement by lamination method would work better than stitching method. Recalls that the glass yarns were laminated and fixed all along the length; one breakage at the joint would cause limited stretch and creep over the length of the breakage. And as long as the rest of the fabric is intact, the dimensional integrity will be held by the rest glass yarns.

Furthermore, there are many other possibilities of improving a PE fabric or any other fabrics used in fabric formwork. First of all, there are other choices of reinforcement materials, such as UHMWPE (Ultra High Molecular Weight Polyethylene), Kevlar, or even carbon fiber. These materials are more expensive than glass yarn but are much stronger and stiffer (Dorey, 1980; Lysenko, Lysenko, Astashkina, & Gladunova, 2011.; Barbero, 2011; Mukhopadhyay, 1993.; Jassal, & Ghosh, 2001.; Karacan, 2005.; Happey, 1983.). If they are used to reinforce PE fabric, the result may turns out to be more cost efficient for the same amount of improvement. Second, the improvement may also be achieved through altering the yarn construction of the woven fabric. The fabric that is woven to have triangular configuration called tri-axial weave has been developed and is reported to have better dimensional stability than traditional warp and

weft woven fabrics (ref). This may work even better than reinforcements since no extra material is added and thus the cost of reinforcement material and reinforcement process is eliminated. Third, the possibility of improving the stability of PE fabric simply by pre stretching before use as mentioned earlier in chapter 3 is also worth investigation because this may be the most convenient and economical method. The questions needed to be answered are: how much strain and how much time are needed to pre-stretch a PE fabric to reduce its IED, by how much? Is the reduction permanent or the effect will diminish when PE fabric recovers it stretch slowly?

Nevertheless, the methods of reinforcement or improvement techniques are infinite and require researchers' interests and effort to continuously seeking better solutions. The two reinforcement methods are tested and compared in this paper for a start.

References

Abdelgader, H., West, M., & Górski, J. (2008). State-of-the-art report on fabric formwork. *Proceedings of the International Conference on Construction and Building Technology, Kuala Lumpur, Malaysia.*

Adanur, S. (1995). Fiber properties and Technology. In Adanur, S. (Eds.), *Wellington sears handbook of industrial textiles*. Lancaster, Pa: Technomic Pub.

Anonymous. (2007). DSM dyneema stays strong in several markets. *Southern Textile News, 63*(24), 8-8.

Al Awwadi Ghaib, M., & Górski, J. (2001). Mechanical properties of concrete cast in fabric formworks. *Cement and Concrete Research, 31*(10), 1459-1465.

ASTM Standard D2256 -10, 2010, "Standard Test Method for Tensile Properties of Yarns by the Single-Strand Method," ASTM International, West Conshohocken, PA, 2012, DOI: 10.1520/D2256_D2256M-10E01, www.astm.org.

ASTM Standard D5034 - 09, 2009, "Standard Test Method for Breaking Strength and Elongation of Textile Fabrics (Grab Test)," ASTM International, West Conshohocken, PA, 2012, DOI: 10.1520/D5034-09, www.astm.org.

ASTM Standard D5262 - 07, 2007, "Standard test method for evaluating the unconfined tension creep and creep rupture behavior of geosynthetics," ASTM International, West Conshohocken, PA, 2012, DOI: 10.1520/D5262-07R12, www.astm.org.

ASTM Standard D6193 - 11, 2011, " Standard Practice for Stitches and Seams," ASTM International, West Conshohocken, PA, 2012, DOI: 10.1520/D6193-11, www.astm.org.

Barbero, E. J. (2011). Chapter 2: Materials. *Introduction to composite materials design*. Boca Raton, FL: CRC Press.

Barbero, E. J. (2011). Chapter 3: Manufacturing Process. *Introduction to composite materials design*. Boca Raton, FL: CRC Press.

Bennett, S., Johnson, D., & Johnson, W. (1983). Strength-structure relationships in PAN-based carbon fibres. *Journal of Materials Science, 18*(11), 3337-3347.

Billner, K. *P.* (1936). Method of and Apparatus for Treating Concrete, U.S. Pat. 2,046,867.

Bindhoff, E. W., & King, J. C. (1982). World's largest installation of fabric-formed pile jackets. *Civil Engineering—ASCE, 52*(3), 68-70.

Concrete Canvas, (2011). Available from: http://www.concretecanvas.co.uk

Delijani, F. (2010). The evaluation of changes in concrete properties due to fabric formwork. Master's thesis, Winnipeg: University of Manitoba.

Dorey, G. (1980). The promise of carbon fibres. *Physics in Technology, 11*, 56.

Fab-Form Industry LTD. (2011). Retreived from: http://www.fab-form.com/index.php

Fung, W. (2002). *Coated and laminated textiles.* Cambrdge: Woodhead Publishing Ltd.

Galiano, L., Frenneth, F., Mostafavi, M. (2003). Arquitectura Viva, 2003, 101–114.

Hall, M. E. (2000). Finishing of technical textiles. In Horrocks, A.R. & Anand, S.C. (Eds.), *Handbook of technical textiles* (152-172). New York: Woodhead Publishing.

Hall, D. M., Adanur, S. Broughton, JR. R. M. & Brady, P. H. (1995). Natural and man-made fibers. In Adanur, S. (Eds.), *Wellington sears handbook of industrial textiles*. Lancaster, Pa: Technomic Pub.

Happy, F. (1983). *Applied fiber science*. London: Academic Press.

Hatch, K. L. (2006). Chapter 18: olefin fibers. *Textile Scince.* Apex: Tailored Text Custom Publishing.

Holzwart, C., Raczkowski, K., & Sturgeon, K. (2010). Fatty Shell: Flexible Formwork. Available from: http://cargocollective.com/fabroboticsnet/Fatty-Shell-Flexible-Formwork

Horrocks, A. R., Anand, S., & Anand, S. (2000). *Handbook of technical textiles.* New York: Woodhead Publishing.

Jassal, M., & Ghosh, S. (2002). Aramid fibres-an overview. *Indian journal of fiber and textile research, 27*(3), 290-306.

Karacan, I. (2005). Structure-property relationships in high-strength high-modulus polyethyelene fibres. *Fibres & Textiles in Eastern Europe, 13*(4), 15-21.

Kawai, K. (1999). Highly oriented polymer fiber and method for making the same. US patent 5965260.

Koerner, R. M., & Welsh, J. P. (1980). *Construction and geotechnical engineering using synthetic fabrics*. New York: Wiley.

Kwolek S. L., (1971). Poly (p-benzamide) composition, process and product. US patent 3600350.

Lamberton, B. (1989). Fabric forms for concrete. *Concrete International, 11*(12), 59-67.

Lawrence, C. A., & Shen, X. (2000). An investigation into the hydraulic properties of needle-punched nonwovens for application in wet-press concrete casting part I: Wet-press concrete casting. *Journal of the Textile Institute, 91*(1), 48-60.

Lemstra, P. J., Bastiaansen, C. W. M., Rastogi, S., & Salem, D. (2000). Basic aspects of solution (gel)-spinning and ultra-drawing of ultra-high molecular weight polyethylene. *Structure Formation in Polymeric Fibers,* , 185-224.

Leflaive, E. (1988). 'The use of natural fibres in geotextile engineering' 1st Indian Geotextile Conference. *Reinforced soil and geotextiles.* 81 - 84.

Lilienthal, L. W. G. (1899). Fireproof Ceiling. U.S. Pat. 619,769.

Linssen, T. (2008). Concrete in a bag. Available from: http://studiothol.nl/concreteinabag.html

Lysenko, A., Lysenko, V., Astashkina, O., & Gladunova, O. (2011). Resource-conserving carbon fibre technologies. *Fibre Chemistry, 42*(5), 278-286.

Malone, P. G. (1999). *Use of permeable formwork in placing and curing concrete.* US: U.S. Army Engineer Research and Development Center.

Manelius, A. M. (2009). Ambiguous chairs cast in fabric formed concrete. Retreived from: http://www.fabricforming.org/images/papers/Anne-MetteManeliusPaperStructuralMembranes.pdf

Marosszeky, M., Chew, M., Arioka, M., & Peck, P. (1993). Textile form method to improve concrete durability. *Concrete International, 15*(11), 37-37.

Miraftab, M. (2000). Technical Fibres. In Horrocks, A.R. & Anand, S.C. (Eds.), *Handbook of technical textiles* (152-172). New York: Woodhead Publishing.

Mitra, B. C. (2002). Synthetic vs. natural geotextiles. *Textile Trends, 45*(8), 39-41.

Mukhopadhyay, S. K. (1993). High performance fibers – glass fiber. *Textile Progress, 25*(3), 36-45.

Mukhopadhyay, S. K. (1993). High performance fibers – carbon fiber. *Textile Progress, 25*(3), 19-36.

Mukhopadhyay, S., Deopura, B. L., & Alagirusamy, R. (2004). Production and properties of high-modulus -- high-tenacity polypropylene filaments. *Journal of Industrial Textiles, 33*(4), 245-268.

Neff,W.(1941). Building construction, U.S. Pat. 2,270,229.

Otto, F., & Nerdinger, W. (2005). Frei otto: Complete works : Lightweight construction, natural design. Basel: Birkhäuser.

Pang, F., Wang, C. H., & Bathgate, R. G. (1997). Creep response of woven-fibre composites and the effect of stitching. *Composites Science and Technology, 57*(1), 91-98.

Parthasarathi, V. (2008). A review on versatility of high performance fibres. *Man-made Textiles in India, 51*(4), 116-121.

Pildysh, M., & Wilson, K. (1983). Cooling ponds lined with fabric-formed concrete. *Concrete International, 5*(09), 32-35.

Pollio, M. V. (1960). *The ten books on architecture* (M. H. Morgan, Trans.). NewYork: Dover. (Original work produced around 15BC)

Pritchard, M., Sarsby, R. W., & Anand, S. C. (2000). Textiles in civil engineering. Part 2 – natural fibre geotextiles. In Horrocks, A.R. & Anand, S.C. (Eds.), *Handbook of technical textiles* (372-406). New York: Woodhead Publishing.

Propex, (2011). Geotex 315ST product data sheet. Retrieved from: http://geotextile.com/downloads/Geotex%20315ST%20Product%20Data%20Sheet.pdf

Rankilor, P. R. (2000). Textiles in civil engineering. part 1. – geotextiles. In Horrocks, A.R. & Anand, S.C. (Eds.), *Handbook of technical textiles* (358-371). New York: Woodhead Publishing.

Remy, T., & Veenhuizen, R. (2010). Concrete chair by Tejo Remy & René Veenhuizen. Available from: http://www.dezeen.com/2010/03/18/concrete-chair-by-tejo-remy-renee-veenhuizen/

Schubel, P. J., Warrior, N. A., & Elliott, K. S. (2008). An investigation into factors affecting the performance of composite controlled permeable formwork liners: Part II – filter medium. *Construction & Building Materials, 22*(11), 2235-2249.

Smith, P., & Lemstra, P. J. (1980). Ultra-high-strength polyethylene filaments by solution spinning/drawing. *Journal of Materials Science, 15*(2), 505-514.

Smith, P., Lemstra, P., Pijpers, J., & Kiel, A. (1981). Ultra-drawing of high molecular weight polyethylene cast from solution. *Colloid & Polymer Science, 259*(11), 1070-1080.

Stein, H. L. (1988). Ultrahigh molecular weight polyethylenes (uhmwpe). *Engineered materialsh handbook*, 2, 167–171.

Sondhelm, W. S., (2000). Technical fabric structures – 1. woven fabrics. In Horrocks, A.R. & Anand, S.C. (Eds.), *Handbook of technical textiles* (358-371). New York: Woodhead Publishing.

Veenendaal, D., West, M., & Block, P. (2011). History and overview of fabric formwork: Using fabrics for concrete casting. *Structural Concrete, 12*(3), 164-177.

Waller, J. H. W., & Aston, A. (1953). Corrugated concrete shell roofs. *ICE Proceedings: Engineering Division, 2* (4),153-182.

West, M. (2007). C.A.S.T. laboratory. *Fabric Architecture, 19*(5), 53.

West, M. (2004). Fabric-formed concrete columns. *Concr.Int., 26*(6), 42-45.

Wu, Z., Zhang, A., Percec, S., Jin, S., Jing, A. J., Ge, J. J., et al. (2003). Structure and properties of melt-spun high acrylonitrile copolymer fibers via continuous zone-drawing and zone-annealing processes. *Thermochimica Acta, 396*(1–2), 87-96.

Appendix A – Statistical Analysis: T test with unequal variance.

Null Hypothesis: no difference among means.

Confidence Level: 95%

Rejecting condition: $t > t_{m, 0.95}$

Elongation		Degrees of Freedom			Hypothesis
Comparing Groups:		m	t	$t_{m, 0.95}$	
L-1000 Vs. O-1000		7.661	1.300	1.895	not rejected
S-1000 Vs. L-1000		7.890	0.727	1.895	not rejected
S-1000 Vs.O-1000		7.929	0.582	1.895	not rejected
L-500 Vs. O-500		7.691	2.702	1.943	Rejected
S-500Vs. L-500		6.831	2.215	1.943	Rejected
S-500Vs.O-500		6.054	4.991	1.943	Rejected

Initial modulus		Degrees of Freedom			Hypothesis
Comparing Groups:		m	t	$t_{m, 0.95}$	
L-1000 Vs. O-1000		5.653	149.448	2.015	Rejected
S-1000 Vs. L-1000		7.240	71.442	2.015	Rejected
S-1000 Vs.O-1000		6.874	90.325	2.015	Rejected
L-500 Vs. O-500		7.628	172.226	1.943	Rejected
S-500Vs. L-500		6.191	73.242	1.943	Rejected
S-500Vs.O-500		7.067	141.562	1.943	Rejected

IED at zero slope		Degrees of Freedom			Hypothesis
Comparing Groups:		m	t	$t_{m, 0.95}$	
L-1000 Vs. O-1000		5.500	29.002	2.015	Rejected
S-1000 Vs. L-1000		6.881	15.961	2.015	Rejected
S-1000 Vs.O-1000		7.027	15.579	2.015	Rejected
L-500 Vs. O-500		5.882	36.364	2.015	Rejected
S-500Vs. L-500		7.337	3.967	2.015	Rejected
S-500Vs.O-500		7.058	30.820	2.015	Rejected

Creep		Degrees of Freedom			
Comparing Groups:		m	t	$t_{m, 0.95}$	
L-1000 Vs. O-1000		7.539	0.929	1.895	not rejected
S-1000 Vs. L-1000		7.857	0.247	1.895	not rejected
S-1000 Vs.O-1000		7.893	0.662	1.895	not rejected
L-500 Vs. O-500		7.985	0.268	1.943	not rejected
S-500Vs. L-500		6.014	2.534	1.943	Rejected
S-500Vs.O-500		5.867	2.116	1.943	Rejected

Appendix B – Statistical Analysis: T test with unequal variance.

Total (MAX) Elongation (mm):		
Loading:	1000N:	
	Without Cork	With Cork
	13.34977	13.80594
	13.72934	13.41726
	13.43173	13.46377
	14.03427	13.94743
	14.16535	14.06403
Ave.	13.742092	13.739686
SD	0.358789303	0.288458991
VAR	0.128729764	0.083208589
2 tailed T-test Value for unequal variance:		0.990975
Conclusion:		**No difference on both means**
Loading:	500N:	
	8.11219	8.05592
	8.09235	8.21334
	7.97428	8.19188
	7.86938	7.90159
Ave.	8.00599	8.21155
SD	8.010838	8.114856
VAR	0.097835053	0.135957129
	0.009571698	0.018484341
2 tailed T-test Value for unequal variance:		0.206027
Conclusion:		**Likely there is a difference and elongation with cork liner is larger**

* Note the standard deviation (SD) is much lower than the SD in group O-1000 and group O-500 samples. This is due to the fact that samples from O-1000 and O-500 were cut from different yarn sets as required for ASTM methods. The samples cut for this sets of tests were cut from the same yarn sets to ensure the samples were as homogeneous as possible because the aim of these tests was to evaluate the difference of elongations of unreinforced samples tested with cork liner and without cork liner.